Transportation Research Part B 117 (2018) 542–572

Contents lists available at ScienceDirect

Transportation Research Part B

journal homepage: www.elsevier.com/locate/trb

An integrated framework for electric vehicle rebalancing and staff relocation in one-way carsharing systems: Model formulation and Lagrangian relaxation-based solution approach

Meng Zhao[a], Xiaopeng Li[c], Jiateng Yin[b,*], Jianxun Cui[d], Lixing Yang[b], Shi An[d]

[a] Institute of Systems Engineering, Dalian University of Technology, Dalian, 116024, China
[b] State Key Laboratory of Rail Traffic Control and Safety, Beijing Jiaotong University, Beijing, 100044, China
[c] Department of Civil and Environmental Engineering, University of South Florida, FL 33620, United States
[d] School of Transportation Science and Engineering, Harbin Institute of Technology, Harbin, 150090, China

ARTICLE INFO

Article history:
Received 31 March 2017
Revised 22 September 2018
Accepted 25 September 2018
Available online 6 October 2018

Keywords:
One-way carsharing system
Electric vehicle rebalancing
Staff relocation
Space-time network
Lagrangian relaxation

ABSTRACT

In one-way electric vehicle (EV) carsharing systems, a practical issue that needs to be addressed is the imbalance of EVs with respect to the spatial time-dependent user reservations at different carsharing stations. In practice, appropriate EV rebalancing operations can satisfy user reservations with limited resources and effectively save system investments. This paper proposes an integrated framework that can determine the optimal allocation plan of EVs and staff on the strategic level while considering the operational EV relocation and staff relocation decisions, in order to minimize the total cost, including the EV and staff investment, EV rebalancing and staff relocation costs. In this framework, the dispatching routes of EVs and staff are represented by two sets of space-time paths in the planning time horizon by using a space-time network representation, and the considered problem is then formulated into a mixed-integer linear programming model (MILP). This model explicitly considers (1) the satisfaction of time-dependent user reservations through dynamically rebalancing EVs and relocating staff to keep the service quality of carsharing system, and (2) the EV battery capacity with limited traveling distance and the charging process of EVs at parking stations. A Lagrangian relaxation-based solution approach is developed to decompose the primal problem into several sets of computationally efficient subproblems. In order to generate good-quality solutions, we also propose a three-phase implementing algorithm based on dynamic programming according to the values of Lagrangian multipliers. An illustrative numerical example and a real-world case study (based on the operation data of Seattle, WA) are conducted to verify the applicability of the formulated model and effectiveness of the proposed approach.

* Corresponding author.
E-mail address: jiatyin@bjtu.edu.cn (J. Yin).

https://doi.org/10.1016/j.trb.2018.09.014
0191-2615/

1. Introduction

The expansion of residents and private vehicles in large cities, such as Beijing, Tokyo and San Francisco, has imposed great pressures on the urban transportation systems. For example, in Beijing, the number of vehicles has increased by about 154 thousand (or 2.8 percent) from 2014 to 2015, and over 65% of these new vehicles are private cars. The number of annual average daily trips (AADT) in downtown area grows to over 28 million and the trips on private vehicles take over 31%. This may well explain the greatly worsened traffic and environmental conditions of Beijing in recent years. To overcome this urgent problem of big cities, one of the promising approaches is the application of carsharing systems, in which a group of people collectively own or use a number of spatially distributed vehicles. There has been abundant evidence that carsharing systems can effectively release the pressure to other public transportation modes, save urban parking space, and reduce air pollution e.g., Jian et al. (2016); Li et al. (2016) and Boyacı et al. (2017).

In general, the current carsharing systems are classified into three patterns according to their different rental modes, which are round-trip, free-floating and one-way carsharing systems, respectively (Becker et al., 2017). For round-trip systems, the origin and destination of each user are restricted to the same parking station. In other words, the users are required to return vehicles to their original stations. Due to this operational constraint, round trip systems are inflexible to many users (e.g., those with one-way trips or relatively long activity durations). In contrast, free-floating systems allow the users to drop the vehicles at any parking port in a predetermined area, which improves user convenience yet causes relatively high fleet management cost (e.g., the costs of collecting and returning the vehicles to relevant facilities)(Firnkorn, 2012; Weikl and Bogenberger, 2015). As a compromise, in one-way carsharing systems, each user can return a vehicle to a different station other than the pickup station, which has better flexibility than round-trip systems yet does not incur as high cost as free-floating systems. In other words, one-way carsharing systems strike a good balance between operation costs and flexibility. Many carsharing organizations such as Zipcar and Car2Go tend to increase the proportion of one-way service pattern in recent years[1][2](Jorge et al., 2015).

An outstanding challenge to one-way carsharing operations is the imbalance of available vehicles at different stations caused by the gravitational effect (Weikl and Bogenberger, 2015) among different areas and the tide phenomena of daily trips (Waserhole et al., 2013), which often lead to vehicle shortage in some stations yet too high vehicle inventories in others. This challenge apparently reduces the service quality of carsharing systems such that some users have to wait for available vehicles. Further, it causes waste of vehicle resources long sitting in particular stations without being used. In practice, an effective strategy to overcome this problem is to properly allocate the vehicles to parking stations at the beginning of operation cycle and timely rebalance the vehicles by a crew of drivers (namely fleet managing staff) (Kek et al., 2009; Smith et al., 2013; Nourinejad et al., 2015). Such staff-based vehicle operations, if not properly managed, may have imbalanced distribution of staff among the parking stations, or even disruptions of carsharing network operations. Hence, it is important to carefully determine the allocations of EVs and staff to parking stations while considering the vehicle rebalancing and staff relocation operations in one-way carsharing systems. In recent years, to further enhance the environmental and social benefits of carsharing systems, electric vehicles (EV) are gradually favored by most carsharing organizations, because EV sharing services are not only efficient but also sustainable (Li et al., 2016; Xu et al., 2017).

Nevertheless, the current studies that simultaneously consider the EVs and staff allocations, EV rebalancing and staff relocation through a systematic view are very few, which is partially due to the following two reasons. (1) On one hand, applying EVs actually brings new challenges to rebalancing of shared vehicles in one-way carsharing systems. Restricted by the limited battery capacity and the existing charging technology, most EVs need a considerable charging time after a limited travel distance or time. Therefore, in EV one-way carsharing systems, the rebalancing of EVs is actually a complicated problem that not only involves the space-time distribution of EVs but also is constrained by the limited battery capacity, which makes it extremely difficult to obtain a global-optimum or near-optimum solution. (2) On the other hand, the EV rebalancing design in one-way carsharing system is essentially a very complicated problem due to the complex coupling relationships among user activities, staff members and EVs. For bicycle sharing systems, the rebalancing of bikes is usually handled by dispatching a fleet of capacitated trucks to maintain the number of bicycles in each station (Dell'Amico et al., 2014; Forma et al., 2015; Zhang et al., 2016). Correspondingly, the relocation problem in EV carsharing systems faces a different kind of challenge since it is practically not suitable to use trucks for the relocation of multiple vehicles due to the complexity and inefficiency of EV loading/unloading process (Bruglieri et al., 2014). Hence, each vehicle rebalancing task in one-way carsharing system is generally achieved by one staff member, which means that we need to precisely capture the spatial-time user activities and then dynamically dispatch the staff members to balance the distribution of EVs (Boyacı et al., 2017). To achieve a global optimum for one-way carsharing systems, more coupling constraints among user activities, EVs and staff members should be rigorously considered, which however enhances the computational intensity for the problem of interest.

To address these above issues, this study first adopts a space-time network to represent the EV rebalancing and staff relocation operations in a one-way carsharing system, and then proposes an integrated framework to determine the optimal numbers of EVs and staff members allocated to each parking station at the beginning of the operation cycle while con-

[1] https://www.bostonglobe.com/business/2014/05/01/zipcar-test-one-way-car-sharing/5WkDIkVEwtK4B2m2CF6NhK/story.html.

[2] https://transportation.arlingtonva.us/carsharing/car2go/.

sidering the operational EV rebalancing and staff relocation decisions. The objective is to minimize the system cost while satisfying all the user reservations to enhance the service quality of carsharing company. Specifically, we formulate the problem into a mixed-integer linear programming (MILP) model that aims to minimize the total investment costs and operation costs of EVs and staff for serving the dynamic origin-destination (OD) reservations. In particular, the developed model is able to capture the practical EV battery capacity limitation and battery recharging process at parking stations. To solve the model more efficiently, we propose a variety of approaches (e.g., Lagrangian relaxation with embedded dynamic programming, branch and bound, and greedy algorithm) that can obtain a near-optimal solution in a shorter computational time compared with state-of-the-art MILP commercial solvers such as CPLEX and Gurobi.

1.1. Literature review

With the increasing concerns on urban congestion and carbon emission problems in recent years, carsharing systems have become an active research area e.g., Barth and Shaheen (2002); Barth et al. (2004); Nair and Miller-Hooks (2011); Furuhata et al. (2013); Boyacı et al. (2015); Schmöller et al. (2015); Hu and Liu (2016); Jian et al. (2016); Li et al. (2016) and Becker et al. (2017). In general, studies in this area can be divided into two levels, i.e., the strategic level and the operational level.

At the strategic level, relevant studies mainly focus on the long-time planning strategies, e.g., the number, capacities, and locations of vehicle parking stations, and the fleet and staff sizes (Correia and Antunes, 2012; Fanti et al., 2014; Hu and Liu, 2016; Li et al., 2016; Xu et al., 2018). For example, Correia and Antunes (2012) developed three mixed integer programming (MIP) models to determine the optimal number, locations and capacities of parking stations with respect to the maximum profits of a one-way carsharing company. Li et al. (2016) proposed a Continuum Approximation (CA) model for the design of one-way carsharing systems in a metropolitan area, which determines the optimal EV station locations and the corresponding fleet sizes to minimize the total cost. Based on the random arrival rates of user reservations that follow a homogeneous Poisson process, Hu and Liu (2016) presented a joint design of station capacities and fleet size for one-way carsharing systems to maximize the system revenue from the perspective of the carsharing operator.

At the operational level, studies concentrate on daily management and operation of vehicles and staff in carsharing networks. In particular, since users are allowed to drop off vehicles at arbitrary parking stations in one-way carsharing systems, the vehicles shall be rebalanced dynamically in order to satisfy the user reservations. The research by Barth and Shaheen (2002) has indicated that, one-way trips in a one-way carsharing system are very likely to cause imbalance of vehicle numbers among different stations. In other words, some carsharing stations may face the vehicle shortage issue while others may be overfilled at the same time. Therefore, a lot of recent studies begin to stress this practical issue for vehicle rebalancing and staff relocation in one-way carsharing systems e.g., Kek et al. (2009); Febbraro et al. (2012); Boyacı et al. (2015); Nourinejad et al. (2015); Weikl and Bogenberger (2015) and Boyacı et al. (2017). For instance, Febbraro et al. (2012) developed a user-based approach to generate the optimal rebalancing strategy by using a discrete event model. This methodology aims to minimize the absolute difference between the number of available vehicles and user reservations in a specified time period. For increasing the profitability of a one-way carsharing company, Jorge et al. (2014) developed two models, i.e., a mathematical model to optimize the vehicle rebalancing operations and a simulation model to study different real-time rebalancing policies. The results indicated that, with appropriate vehicle rebalancing operations, the profits of a carsharing company can be evidently improved. Nevertheless, a practical issue for vehicle rebalancing is that, each vehicle rebalancing task must be achieved by at least one staff member. Thus, vehicle rebalancing operations actually require a systemic and rigorous operational plan that considers both the vehicle rebalancing and staff relocation simultaneously. More recently, some studies have addressed this practical significant yet theoretically challenging problem through the integration of vehicle rebalancing and staff relocation. Kek et al. (2009) proposed a three-phase optimization-trend-simulation approach, in which the first phase is to generate a set of near-optimal vehicle rebalancing strategies, the second phase is to convert the optimized result into a series of practical operating parameters (e.g., staff activities, rebalancing technique, rebalancing thresholds), and the last phase evaluates the effectiveness of the operating parameters by simulation. In order to jointly optimize the vehicle rebalancing and staff relocation strategies, Nourinejad et al. (2015) developed an integrated mathematical model, in which the rebalancing trajectories of vehicles and staff were formulated as two sets of decision variables and the aim is to minimize the total cost of a carsharing company. Due to the complexity of the formulated model, a heuristic algorithm was developed to find a feasible solution within an acceptable solution time.

Since EVs are becoming much more indispensable in the future development of green and intelligent transportation systems, it is practically desirable to consider EV rebalancing problem in carsharing systems. Different from conventional vehicles, the challenging issue that distinguishes this problem with traditional vehicle rebalancing problem is the limitation of EV battery capacity and considerable battery charging time. Weikl and Bogenberger (2015) focused on the EV rebalancing problem in a free-floating carsharing system, where a practice-ready relocation model for free-floating carsharing systems with conventional and electric vehicles was introduced to maximize the total profits of carsharing company. To solve this model more efficiently with low computational time, the solution was obtained through a two-level-procedure algorithm, in which the upper level aims to generate the optimal inter zone relocation outlet, and the lower level controls the detailed vehicle serving and recharging processes based on a series of heuristic rules. Finally, three sets of experiments for free-floating systems in Munich are performed to demonstrate its effectiveness. In one-way EV carsharing systems, Boyacı et al. (2017) recently developed an integrated multi-objective mixed integer linear programming model and a discrete event

simulation framework for the optimal design of EV rebalancing and staff relocation with users' reservations. In particular, a concept of safety gap was proposed to improve the robustness of the operation strategies under stochastic user delay and traffic congestion condition. Due to the complexity of the model, a clustering procedure based optimization framework was designed to simultaneously determine the station clustering, EV rebalancing and staff relocation strategies. The obtained solution was then given as input to an event-based simulator for testing its feasibility in terms of EV recharging requirements. A good solution that balances the efficiency and accuracy can be finally generated by iteratively repeating this process and adding new EV recharging constraints. Then, a lot of computational experiments based on the real-world data of Nice, France were implemented, which illustrate the effectiveness of the proposed approach and also derive several meaningful insights with respect to the operational strategies in one-way carsharing systems.

1.2. Focus of this study

As stated above, a variety of models and approaches with respect to vehicle rebalancing issues have been proposed for improving the operational efficiency in carsharing systems. Nevertheless, to the best of our knowledge, only a small number of recent developments have tried to integrate the vehicle and staff allocation designs for EV one-way carsharing systems with the consideration of vehicle and staff dispatching plans. In the methodological aspects, there is fewer study that proposes an exact mathematical model or attempts to solve the true optimal solution for this strategic optimization design problem. The existing approaches solving EV rebalancing and staff relocation problem usually simplify or neglect a part of practical factors, such as dynamic spatiotemporal reservations, limited EV battery capacity and noticeable EV charging time, and most of these formulations are solved by heuristic algorithms or computer simulation. For example, Nourinejad et al. (2015) proposed a discrete-event continuous time model that formulated the joint vehicle rebalancing and staff relocation problem into two integrated multi-traveling salesman formulations. Note that this model considers the conventional vehicle rebalancing problem with unlimited vehicle traveling distance, and heuristic algorithms incorporated with commercial optimization solvers were developed to circumvent the computational burden from dynamic spatiotemporal reservations. Boyacı et al. (2015) considered a one-way EV sharing system that takes into account the EV relocation and recharging requirements. To decrease the complexity of the proposed model, the charging period of the EV is simplified as a fixed period of time dwelling in the station after completing a user reservation. More recently in Boyacı et al. (2017), a series of hard constraints, such as station and vehicle capacity limitations are considered in the mathematical formulations. In order to solve these models efficiently, the EV battery capacity and charging constraints are simplified in the optimization procedure. Instead, a simulation module is developed to evaluate the feasibility of the obtained solutions. While these approaches can return reasonable vehicle rebalancing solutions within an acceptable time, the systematic optimality of the whole framework is not explicitly discussed, and there lacks theoretically benchmarks to evaluate the performance of these solutions with respect to the true optimum.

In this study, we address the strategic planning problem in an EV carsharing system to determine the optimal allocation plan of EVs and staffs to parking stations while considering the operational EV relocation and staff rebalancing decisions (termed as EVSR in the following content). We formulate this EVSR problem into an exact mathematical model that explicitly considers the spatial time-dependent user reservations, limited EV battery capacity and EV charging time. New methodologies are introduced to solve the exact optimal solution or a near-optimum solution with an optimality gap assurance. Specifically, this paper aims to make the following contributions to the literature.

(1) By using a space-time network representation, the EV rebalancing and staff relocation operations are represented by two sets of space-time paths in the discrete time horizon. This method enables to guarantee that the spatial time-dependent user reservations can be served through dynamically rebalancing EVs and relocating staff members. Meanwhile, in order to explicitly depict the EV battery capacity limitation and its recharging processes, we particularly denote a time-dependent state for each vehicle to model the EV battery volume variation in the space-time network. Then, the EVSR problem is rigorously formulated into an integer programming model that can be transformed into an equivalent mixed-integer linear programming (MILP) model. Specifically, the aim of the formulated model is to minimize the total investment (i.e., EV purchasing and staff hiring) cost and operation (i.e., EV rebalancing and staff relocating) cost while serving the user reservations as many as possible. Since EVSR problem is properly formulated as a MILP model, it can be solved to the exact optimum with commercial solvers for small or medium instances.

(2) To improve the computational efficiency for solving large-scale instances, we especially propose a variety of approaches combing Lagrangian relaxation with embedded dynamic programming, branch-and-bound and greedy algorithm in order to solve the developed model to near-optimality in an acceptable time. In specific, we dualize two sets of hard constraints in the primal model, which couple the EV and staff space-time paths to the objective function through introducing different Lagrangian multipliers. The relaxed model is then decomposed into a series of resource constrained shortest path (RCSP) problems, traditional shortest path (SP) problems and semi-assignment (SA) problems. To improve the solution quality, we further propose a three-phase implementing algorithm based on dynamic programming that adjusts the solution of the relaxed model into a feasible solution according to the value of Lagrangian multipliers. The proposed algorithm is shown capable of solving large-scale EVSR instances into the exact optimum or a near optimal solution with an explicit small optimality gap.

The reminder of this paper is organized as follows. In Section 2, we present the detailed description for the EVSR problem. Section 3 formulates the EVSR problem into a mixed-integer programming model to generate the optimal EV and

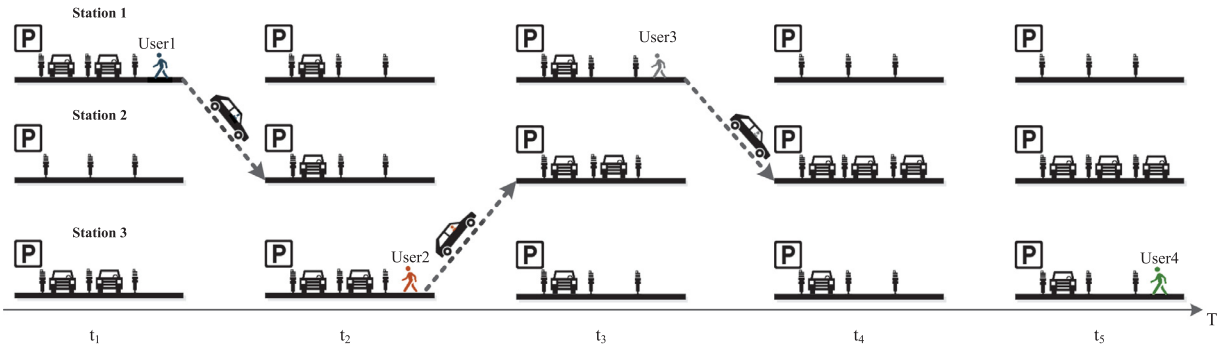

(a) Operation without EV rebalancing (At least 4 EVs are required)

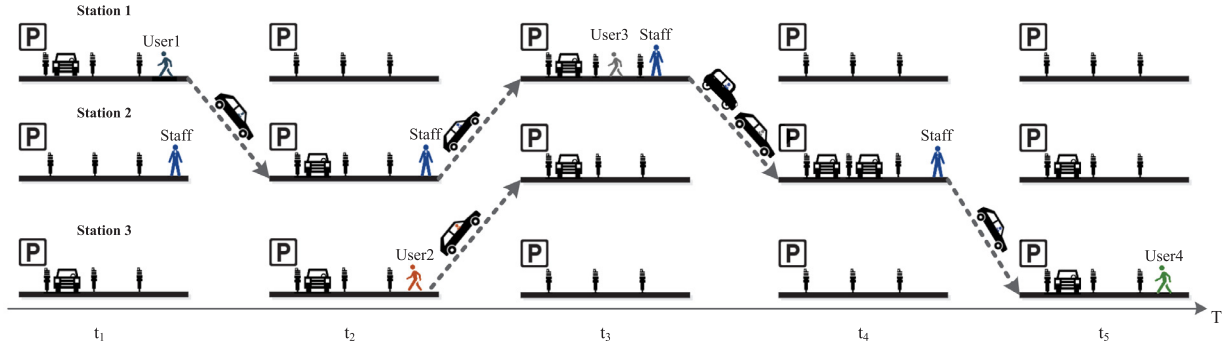

(b) Operation with EV rebalancing (2 EVs and 1 staff member are required)

Fig. 1. Illustration for the operation process of one-way carsharing system.

staff allocation plan while considering the EV rebalancing and staff relocation operations in the considered time horizon. Then, we propose the Lagrangian-relaxation based algorithmic framework for solving the developed model in Section 4. In Section 5, we conduct a series of numerical examples to test the performance of the proposed model and customized solution approach. Finally, conclusions and further studies are presented in Section 6.

2. Problem statement

In the following discussion, we first introduce the EVSR problem in Section 2.1. Then, we present an integrated EVSR framework by using a space-time network representation in Section 2.2.

2.1. EVSR problem in one-way carsharing systems

Consider a one-way carsharing system that operates the services using EVs among a number of predetermined stations located in an urban area. At the beginning of the operation cycle (e.g., each single day), each parking station is initially allocated with a certain number of EVs and staff members, leading to the EV investment cost and staff hiring cost. During the operational phase, users are allowed to visit any parking station according to their reservations to pick up an EV and drop it to another one. Due to the heterogenous space-time distribution of user reservations, the staff members are required to dynamically dispatch the EVs to parking stations with higher demands to prevent the imbalance of EVs among the parking stations, which is called the EV relocation and staff rebalancing operations or dispatching strategies of EVs and staff. Although these EV relocation and staff rebalancing operations require additional costs for the travelling of EVs and staff members, the investment cost can be noticeably compressed with appropriate EV and staff dispatching strategies to serve the user reservations. In this sense, the EVSR problem in our study aims to answer the following question: *how many EVs and staff members are required in a one-way carsharing system and how to allocate these EVs and staff members to each station such that the user reservations can be satisfied with minimum cost by considering the operational EV relocation and staff rebalancing decisions in parallel.*

An illustrative example is shown by Fig. 1, which presents a one-way carsharing system consisting of three EV stations and four user reservations. Here, we consider five time intervals and four reservations where the users plan to pick up the vehicles at time t_1, t_2, t_3 and t_5, respectively. If there is no rebalancing operation for these EVs (shown as Fig. 1(a)), it is obvious that at least 4 EVs are required to fulfil these four user reservations. At time t_5, three of the EVs will be parked

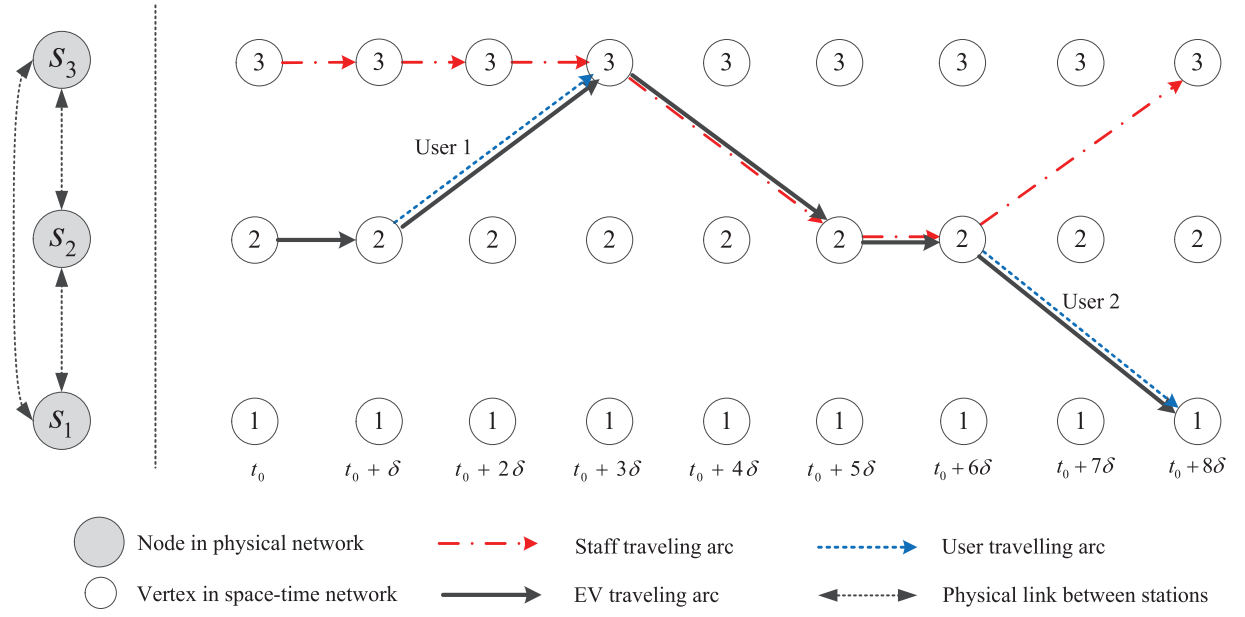

Fig. 2. Representation for EV relocation and staff rebalancing operations in the space-time network.

at parking station 2, which actually causes the imbalance and low utilization of EVs. Alternatively, if we hire only one staff member with appropriate EV relocation strategies (as show in Fig. 1(b)), all these four user reservations can still be covered by initially allocating two EVs and one staff member at parking station 1,3 and 2, respectively. The staff member first drives the EV from parking station 2 to 1 at time t_2, then travels back to parking station 2, and finally rebalances the EV from parking station 2 to 3. This is evidently a much more flexible and economical strategy compared with purchasing four EVs to fulfil these four user reservations.

Therefore, the EVSR problem studied in this paper aims to design the optimal allocation plan of EVs and staff members to uncapacitated parking stations with consideration of optimized EV rebalancing and staff relocation operations to guarantee that (1) the spatial time-dependent user reservations are satisfied; (2) each EV rebalancing task must be operated by one staff member; (3) each EV has a limited battery capacity and must be recharged after a certain traveling distance; (4) the total cost, including the EV and staff investment costs, EV rebalancing cost and staff relocation cost, is to be minimized.

2.2. Space-time network representation

The space-time network, which aims to integrate physical transportation networks with the time-dependent trajectories of objects (such as vehicles or travelers) to particularly capture their spatial and temporal characteristics, is widely utilized in transportation network modeling literature (see Kliewer et al. (2006); Steinzen et al. (2010); Yang and Zhou (2014); Li et al. (2015); Tong et al. (2015); Mahmoudi and Zhou (2016); Zhang et al. (2016), Boland et al. (2017) and Zhang et al. (2017)). For instance, to overcome the bicycle repositioning problems, Zhang et al. (2016) proposed a multi-commodity time-space network flow model, which is transformed into an equivalent MILP model and solved by a heuristic algorithm. Based on a state-space-time network, Mahmoudi and Zhou (2016) effectively solved the vehicle routing problem with pickup and delivery time windows. More recently, by using the time-expanded space-time networks, Boland et al. (2017) developed an efficient dynamic discretization discovery algorithm for the continuous-time service network design problem, which demonstrates that an optimization problem defined on a partial time-expanded network can be solved to the optimality without ever generating the complete time-expanded network.

Consider a directed, connected traffic network (N, A), where N is a finite set of nodes that represent the parking stations of EVs, and E is a finite set of traffic links between any two stations. Since the EVSR problem essentially determines the positions of the studied EVs and staff all the time, the formulation of space-time network is actually appropriate for depicting the space-time trajectories of the EVs and staff. To extend the network into a space-time network, the considered time horizon is primarily discretized into a set of timestamps, denoted by $\mathbf{T} = \{t_0, t_0+\delta, \cdots, t_0+M\delta\}$ with the same time interval δ between each two adjacent timestamps. Here, note that δ is assumed to be properly set such that all the trips (including user trips, EV relocation trips and staff rebalancing trips) start and end at times as integer multipliers of δ.

The example shown in Fig. 2 demonstrates the space-time network formulation of an EV rebalancing and staff relocation process. We can see that a physical carsharing system with three parking stations is shown on the left side. On the right side, a space-time network, which involves 9 timestamps, denoted by $t_0, t_0+\delta, \cdots, t_0+8\delta$, is constructed. Each node in the space-time network represents the state of corresponding parking station at the current timestamp. Particularly, we adopt

three kinds of traveling arcs in the constructed space-time network, which are denoted by the red dashed line, the black solid line and the blue dot line, to represent the space-time trajectories of the staff, EVs and users, respectively. Specifically, these three kinds of space-time arcs in this figure are listed in detail as follows:

(1) User traveling arc. User 1 picks up a vehicle from parking station s_2 at time $t_0+\delta$ and drops it to parking station s_3 after traveling two time intervals. Similarly, user 2 picks up a vehicle from parking station s_2 at time $t_0+6\delta$ and drops it to parking station s_1 two time intervals later.

(2) EV traveling arc. Here, the EV traveling arcs involve waiting arcs (e.g., $(s_2, t_0, s_2, t_0+\delta)$) and activity arcs that are driven by either users (e.g., $(s_2, t_0+\delta, s_3, t_0+3\delta)$) or staff members (e.g., $(s_3, t_0+3\delta, s_2, t_0+5\delta)$).

(3) Staff traveling arc. Similarly, the staff traveling arcs also involve waiting arcs and activity arcs. Particularly, besides the EV rebalancing trips (e.g., space-time arc $(s_3, t_0+3\delta, s_2, t_0+5\delta)$), the staff are sometimes dispatched from one station to another without an EV (e.g., space-time arc $(s_2, t_0+6\delta, s_3, t_0+8\delta)$), where additional expenses will occur to compensate the staff traveling cost, i.e., the staff relocation cost.

3. Model formulation

In this section, we first state the basic assumptions that enable a compact model formulation while capturing the essence of EVSR operations. Then we introduce the parameters, notations and decision variables. Finally, a mix-integer linear programming (MILP) model is rigorously formulated for the EVSR problem.

3.1. Model assumptions

Assumption 1. We assume that the user reservations in our study are treated as dynamic and deterministic activities that are given before the operation phase (e.g., three hours or one day), indicating that the users will not cancel or delay their reservations. In this sense, the dynamic user reservations are essentially captured by the spatial time-dependent OD data in one typical day. Similar assumption is also adopted in Correia and Antunes (2012) and Jorge et al. (2015).

Assumption 2. Our study assumes that the one-way carsharing system is strategically well designed according to the general demand distribution and long-time demand variation properties, which means that the station locations are known in advance and station capacities are sufficient to serve all these user reservations. In other words, the proposed EVSR formulation is based on undersaturated conditions in terms of user demand for the one-way carsharing system. In addition, the parking piles equipped in each parking station are also assumed sufficient and EVs can be recharged as soon as they dwell in the parking station.

Assumption 3. In order to simplify the problem without generality, we assume that all the EVs are in the same working condition. Specifically, all the EVs are homogeneous vehicles that share the same battery capacity and battery consuming rate. Additionally, all parking stations are equipped with identical battery chargers that yield the same charging rate to the parked EVs.

3.2. Parameters and notations

For the convenience of the readers, we first introduce the mathematical notations as follows.

$\mathbf{A}$	Set of space-time arcs in the space-time network
$\mathbf{F}=\{1,2,\cdots,F_{\max}\}$	Set of staff members in the carsharing system
$\mathbf{H}=\{1,2,\cdots,H_{\max}\}$	Set of EVs in the carsharing system
$\mathbf{I}$	Set of parking stations in the carsharing system
$\mathbf{L}$	Set of direct links between parking stations.
$\mathbf{T}$	Set of timestamps in the considered planning time horizon
$\mathbf{V}$	Set of space-time vertexes in the space-time network
f	Index of staff members, $f\in\mathbf{F}$
h	Index of EVs, $h\in\mathbf{H}$
i, j	Index of EV parking stations, $i, j\in\mathbf{I}$
t, s	Index of different timestamps, $t, s\in\mathbf{T}$
(i, j)	Index of direct links between parking stations, $(i, j)\in\mathbf{L}$
(i, t), (j, s)	Index of space-time vertexes, (i, t), $(j, s)\in\mathbf{V}$
(i, t, j, s)	Index of space-time arcs, $(i, t, j, s)\in\mathbf{A}$
$H_{\max}$	Maximum number of EVs
$F_{\max}$	Maximum number of staff members
c^d_{ij}	Staff relocation cost on link (i, j)
c^a	Amortized cost of an EV
c^l_{ij}	EV traveling cost on link (i, j)
c^y	Hiring cost of a staff member

N_{itjs} Number of the user trips on space-time arc (i, t, j, s)
E_0 EV battery capacity
E^+ EV battery charging rate
E^- EV battery consuming rate

We first need to determine the initial numbers of EVs and staff allocated to each parking station at the beginning of operation cycle, and then generate the EV relocation and staff rebalancing strategies at each timestamp. Therefore, the following decision variables are defined to specify this problem.

H_i Initial number of EVs allocated at station i (nonnegative integer variable)
F_i Initial number of staff members allocated at station i (nonnegative integer variable)
$X^h_{it\,js}$ Space-time arc selection indicator, =1 if vehicle h travels on space-time arc (i, t, j, s); =0, otherwise;
$Z^f_{it\,js}$ Space-time arc selection indicator, =1 if staff member f travels on space-time arc (i, t, j, s); =0, otherwise;
U^h_t EV state indicator, =1 if vehicle h dwells at station i at timestamp t; =0, otherwise;
E^h_t Battery volume of vehicle h at timestamp t (nonnegative variable).

Here, it is clear that both the waiting arcs and activity arcs of EVs can be denoted by the set of variables $\{X^h_{it\,js}\}_{(i,t,j,s)\in\mathbf{A},h\in\mathbf{H}}$, explicitly given by $\{X^h_{it\,js}\}_{i=j\vee(i,t,j,s)\in\mathbf{A},h\in\mathbf{H}}$ and $\{X^h_{it\,js}\}_{i\neq j\vee(i,t,j,s)\in\mathbf{A},h\in\mathbf{H}}$, respectively. Similarly, the waiting arcs and activity arcs of staff can also be denoted by the set of variables $\{Z^h_{it\,js}\}_{(i,t,j,s)\in\mathbf{A},h\in\mathbf{H}}$.

3.3. Mathematical model

3.3.1. Systematic constraints

In this part, a series of constraints will be developed to satisfy the systematic requirements of the carsharing company and users. In particular, to represent the traveling trajectories of EVs and staff in the space-time network, we denote two sets of space-time flow constraints that enable to generate the feasible space-time paths of EVs and staff, respectively. Then, we also develop several sets of coupling constraints to guarantee that all user reservations are fulfilled, the EVs are rebalanced by enough staff members, and battery volumes of EVs are adequate on the corresponding space-time travelling arcs. In detail, the involved constraints are formally formulated as follows.

(1) Fleet and staff size constraints

In the strategic design of one-way carsharing systems, the primarily task is to determine the numbers of EVs and staff that are allocated to each station at the beginning of the operating cycle, which is termed as allocation plan. The following constraints first set the upper bound for the total number of EVs and staff members, i.e.,

$$\sum_{i\in\mathbf{I}} H_i \le H_{max}, \tag{1}$$

$$\sum_{i\in\mathbf{I}} F_i \le F_{max}, \tag{2}$$

where H_i and F_i are decision variables that denote the initial numbers of EVs and staff members allocated to each parking station i at initial time t_0. $H_{\max}$ and $F_{\max}$ are parameters that respectively denote the maximum numbers of EVs and staff, which can be set as relatively large numbers in the optimization process. For example, we can set $H_{\max}=4$ in the illustrative example in Section 2.1. Then, by optimizing the EVSR model, the number of required EVs and staff members can be finally determined by considering EV rebalancing and staff relocation operations to save the total cost. In other words, the number of required EVs and staff members given by $H_{en}=\sum_{i\in\mathbf{I}}H_i$ and $F_{en}=\sum_{i\in\mathbf{I}}F_i$ are actually no more than the maximum numbers of EVs and staff, i.e., $H_{\max}\ge H_{en}$ and $F_{\max}\ge F_{en}$. As can be seen from Fig. 3, the maximum numbers of EVs and staff are both set as 5, while only two staff members and two vehicles are actually needed for accomplishing the user trips. Hence, the total investment cost of EVs and staff can be evidently reduced if we can properly design the allocation plan and relocation strategies of EVs and staff members in a one-way carsharing system.

(2) EV space-time flow constraints

In essence, the EV rebalancing problem is to construct a space-time path for each EV, such that the balance of EV numbers among parking stations can be maintained associated with the spatial time-dependent user reservations. Here, we consider the space-time network flow balance constraints of EVs, which ensure to generate a feasible space-time path for each EV $h\in\mathbf{H}$ in the space-time network (see Yang and Zhou (2014) and Mahmoudi and Zhou (2016)), i.e.,

$$\sum_{(j,s)\in\mathbf{V}:(i,t,j,s)\in\mathbf{A}} X^h_{it\,js} - \sum_{(j,s)\in\mathbf{V}:(j,s,i,t)\in\mathbf{A}} X^h_{jsit} \begin{cases} =1, & (i,t)=(i_O,t_O)\\ =-1, & (i,t)=(i_D,t_D),\\ =0, & \text{otherwise.}\end{cases} \quad \forall h\in\mathbf{H},\ (i,t)\in\mathbf{V}, \tag{3}$$

in which (i_O, t_O) and (i_D, t_D) are defined as the dummy origin and dummy destination, respectively. Moreover, we assume that the distances and travel times between dummy origin (or destination) node and the physical nodes are 0.

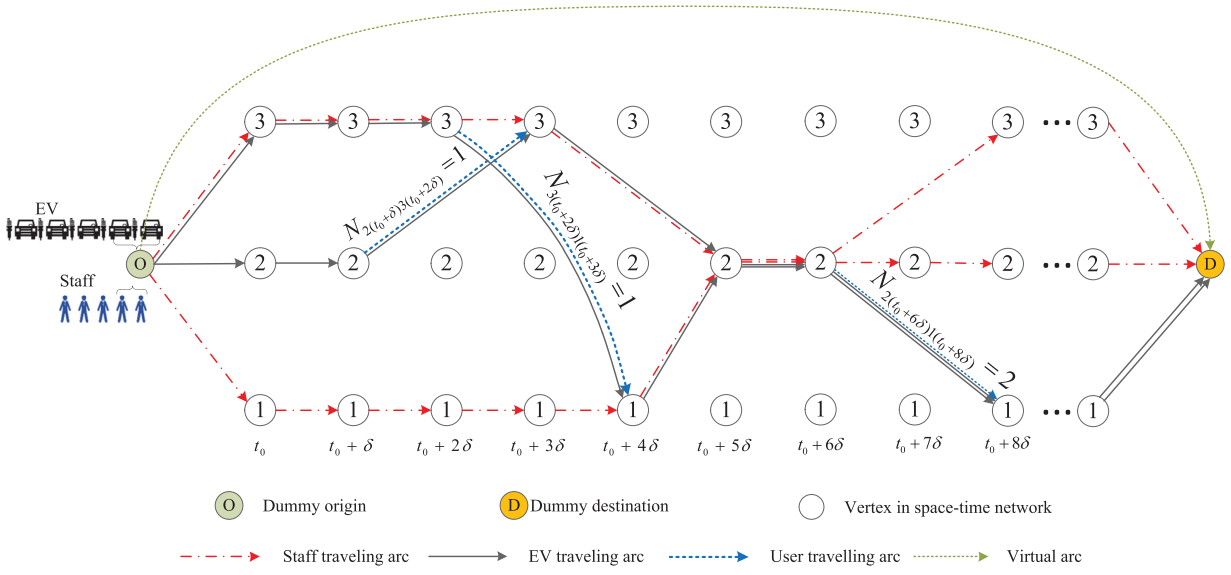

Fig. 3. Illustration for allocation and dispatching strategies of EVs and staff.

Remark 3.1. In particular, we note that, the above constraints essentially define two different scenarios for the EV allocation plan in a one-way carsharing system. The EVs that are not allocated to any parking stations will travel from the dummy origin to dummy destination directly through the virtual arc that connects them, while the others are allocated to their corresponding parking station i at the initial time t_0. An illustration is shown in Fig. 3, in which we see that, only two EVs are dispatched to station 2 and 3 from the dummy origin, while the others are actually not needed in this case and they will travel from dummy origin to dummy destination directly.

Moreover, we let the following constraints denote the relationships between the number of allocated EVs and their dispatching routes at the dummy origin:

$$\sum_{h\in\mathbf{H}} X^h_{i_0 t_0 i t_0} = H_i, \quad \forall i \in \mathbf{I}, \tag{4}$$

in which $X^h_{i_0 t_0 i t}$ determines if vehicle h is allocated to station i at initial time t_0.

(3) User reservation fulfilment constraints

In a one-way carsharing system, the satisfaction of user reservations is critical for the service quality of the carsharing company, which requires that there are always enough EVs in the parking stations for the user reservations. To represent the dynamic passenger demands, we use N_{itjs} to denote the number of users who reserve to pick up EVs from parking station i at time t, and drop them to parking station j at time s (see Fig. 3). The following constraints are formulated to cover the user reservations on each time-dependent travel arc $(i, t, j, s) \in \mathbf{A}$, i.e.,

$$\sum_{h\in\mathbf{H}} X^h_{it js} \geq N_{it js}, \quad \forall (i,t,j,s) \in \mathbf{A}. \tag{5}$$

Constraints (5) indicate that, if a total number of N_{itjs} users reserve to travel through space-time arc (i, t, j, s), the number of EVs traveling through this arc $\sum_{h\in\mathbf{H}} X^h_{it js}$ shall be higher than that. As shown in Fig. 3, the user traveling arcs (e.g., two reservations on arc $(2, t_0+6\delta, 1, t_0+8\delta)$) are all covered by the corresponding EV traveling paths. In this sense, all the user reservations can be fully satisfied by this set of constraints. In particular, it is clear that there may be some other EVs traveling on this arc (the number is represented as $\sum_{h\in\mathbf{H}} X^h_{it js} - N_{it js}$), which are actually the rebalancing trips of EVs operated by staff and will be stressed in the following constraints.

(4) Staff space-time flow constraints

Meanwhile, we note that each EV rebalancing task should be carried out by the corresponding staff member, who will drive the EV to the preferred parking station. The following constrains are defined to represent that each EV rebalancing operation must be carried out by at least one staff member:

$$\sum_{f\in\mathbf{F}} Z^f_{it js} \geq \sum_{h\in\mathbf{H}} X^h_{it js} - N_{it js}, \quad \forall (i,t,j,s) \in \mathbf{A}_r. \tag{6}$$

where $\mathbf{A}_r = \{(i,t,j,s) \in \mathbf{A} \backslash \{(i_O, t_O, i, t_O), (i, t_D, i_D, t_D), (i, t, i, t+\delta)\} | i \in \mathbf{I}\}$ represents the set of space-time arcs where the EV needs to be driven by staff or user. The left side of constraints (6) denotes the number of traveling staff on this arc, and the right side, as we have mentioned above, represents the number of rebalanced EVs on space-time arc (i, t, j, s).

In addition, we also need to consider the space-time trajectories of staff, which are also subject to the space-time balance constraints. Similar to the space-time flow balance constraints of EVs, we employ the space-time flow balance constraints of the staff as follows.

$$\sum_{(j,s)\in\mathbf{V}:(i,t,j,s)\in\mathbf{A}} Z^f_{it\,js} - \sum_{(j,s)\in\mathbf{V}:(j,s,i,t)\in\mathbf{A}} Z^f_{jsit} \begin{cases} = 1, & (i,t) = (i_O, t_O) \\ = -1, & (i,t) = (i_D, t_D), \\ = 0, & \text{otherwise.} \end{cases} \quad \forall f \in \mathbf{F},\ (i,t) \in \mathbf{V}. \tag{7}$$

Similarly, the relationship between the number of allocated staff members and their dispatching routes at the dummy origin is represented by the following constraints:

$$\sum_{f\in\mathbf{F}} Z^f_{i_O t_O i t_O} = F_i, \quad \forall i \in \mathbf{I}. \tag{8}$$

Remark 3.2. In particular, constraints (6) also indicate that, there are still some staff that would have to travel through arc (*i, t, j, s*) without EVs and the number of these traveling trips is represented as $\sum_{f\in\mathbf{F}} Z^f_{it\,js} - \sum_{h\in\mathbf{H}} X^h_{it\,js} + N_{it\,js}$. Inherently, this will cause an extra cost for the staff traveling (i.e., the relocation cost), which we will consider in the objective function in the following content, and we will also analyze this point in the experimental section. Besides, since we focus on the overall optimal design of EVSR problem in the one-way carsharing systems, the microscopic traffic condition, such as the trip modes and variable trip times of staff relocation among stations, are not explicitly analyzed, and we consider that the operations of EV rebalancing and staff relocation consume the same number of time intervals.

(5) EV battery capacity constraints

Finally, we consider the EV battery capacity constraints. Due to the current battery technology, the EVs need to dwell in a parking station for a duration of charging time after a certain travel distance. For simplicity, this study has assumed that all the EVs are fully charged at the initial time t_0 with battery capacity E_0. Here, we particularly define two sets of intermediate variables $\{U^h_t\}_{h\in\mathbf{H},\ t\in\mathbf{T}}$ and $\{E^h_t\}_{h\in\mathbf{H},\ t\in\mathbf{T}}$ to denote the real-time operation state and battery volume of an EV, respectively. Initially, the relationship between binary variables $\{U^h_t\}$ and $\{X^h_{it\,js}\}$ is represented as

$$U^h_t = \sum_{i\in\mathbf{I}} X^h_{it\,it'}, \quad \forall h \in \mathbf{H},\ t,\ t' \in \mathbf{T},\ t' = t + \delta. \tag{9}$$

Constraints (9) indicate that, $U^h_t = 1$ if vehicle h is parked in a station starting from time t; and $U^h_t = 0$ otherwise.

Then, we consider the real-time battery volume variations of EVs in the space-time network. Let E^+ and E^- denote the charging rate and consuming rate of EVs, respectively. Specifically, when vehicle h is traveling between two stations, we obtain that $U^h_{t-1} = 0$, and its current battery volume E^h_t at time t is given by $E^h_t = E^h_{t-1} - E^-$. On the other hand, if vehicle h is dwelling at a parking station, we have $U^h_{t-1} = 1$, and its current battery volume E^h_t at time t is given by $E^h_t = \min\{E^h_{t-1} + E^+, E_0\}$, which indicates that the battery volume of EVs at time t cannot exceed the battery capacity E_0. In summary, we derive the relationship between variables $\{E^h_t\}$ and $\{U^h_t\}$ as

$$E^h_t = \min\{E^h_{t-1} - E^- + (E^+ + E^-)U^h_{t-1}, E_0\}, \quad \forall h \in \mathbf{H},\ t \in \mathbf{T}\backslash\{t_0\}. \tag{10}$$

Besides, we also need to guarantee that all the EVs are fully charged at the initial time t_0 and the battery volume of each EV is always nonnegative during the remaining time, i.e.,

$$E^h_t = E_0, \quad \forall h \in \mathbf{H},\ t = t_0, \tag{11}$$

and

$$E^h_t \geq 0, \quad \forall h \in \mathbf{H},\ t \in \mathbf{T}\backslash\{t_0\}. \tag{12}$$

Note that the above nonlinear constraints (10) can be further reformulated into equivalent linear constraints as

$$E^h_t \leq E_0, \qquad \forall h \in \mathbf{H}, t \in \mathbf{T}\backslash\{t_0\}, \tag{13}$$

and

$$E^h_t \leq E^h_{t-1} - E^- + (E^+ + E^-)U^h_{t-1}, \qquad \forall h \in \mathbf{H}, t \in \mathbf{T}\backslash\{t_0\}. \tag{14}$$

Since the EVRS model aims at minimizing the total operation cost, the EVs always prefer to choose a traveling rout that maintains higher charging level and serve more user reservations. That is, variables $\{E^h_t\}_{h\in\mathbf{H},t\in\mathbf{T}\backslash\{t_0\}}$ will always take the minimum value of E_0 and $E^h_{t-1} - E^- + (E^+ + E^-)U^h_{t-1}$. Therefore, inequations (13) and (14) are able to equivalently represent constraints (10).

3.3.2. Objective function

In our study, the objective function of EVSR contains two parts. The first part is the investment cost for purchasing EVs and hiring staff, i.e.,

$$C_{INV} = c^a \sum_{i\in\mathbf{I}} H_i + c^y \sum_{i\in\mathbf{I}} F_i, \tag{15}$$

in which $\Sigma_{i\in\mathbf{I}}H_i$ and $\Sigma_{i\in\mathbf{I}}F_i$ are the total numbers of utilized EVs and staff, and c^a and c^y denote the unit cost for purchasing an EV and hiring a staff member, respectively. The second part of objective function refers to the operation expenses, including the EV traveling cost and staff relocation cost. In particular, we also denote c^l_{ij} for each $(i, j)\in\mathbf{L}$ to represent the traveling cost of each EV from station i to station j, and c^d_{ij} for each $(i, j)\in\mathbf{L}$ to denote the staff relocation cost from station i to station j, which is essentially the staff traveling expenses without driving EVs. Then, the operation cost of interest is formulated as follows.

$$C_{OP} = \sum_{(i,t,j,s)\in\mathbf{A}}\sum_{h\in\mathbf{H}} c^l_{ij}X^h_{it\,js} + \sum_{(i,t,j,s)\in\mathbf{A}} c^d_{ij}\Big(\sum_{f\in\mathbf{F}} Z^f_{it\,js} - \sum_{h\in\mathbf{H}} X^h_{it\,js} + N_{it\,js}\Big). \tag{16}$$

In the above objective function, $\sum_{h\in\mathbf{H}} c^l_{ij}X^h_{it\,js}$ is the EV traveling cost on each space-time arc $(i, t, j, s)\in\mathbf{A}$, and $c^d_{ij}(\sum_{f\in\mathbf{F}} Z^f_{it\,js} - \sum_{h\in\mathbf{H}} X^h_{it\,js} + N_{it\,js})$ represents the staff relocation (i.e., staff traveling without EVs) cost on each space-time arc $(i, t, j, s)\in\mathbf{A}$.

Remark 3.3. It is worth mentioning that, these two objectives, i.e., investment and operation costs in (15) and (16) are inter-dependent in the optimization of EVSR. For instance, the growth of fleet size surely increases the investment cost for purchasing more EVs, but it shall decrease the operation cost since fewer rebalancing tasks are needed to satisfy the user reservations. In contrast, decreasing the fleet size will correspondingly increase the operation cost, resulting more frequent rebalancing tasks for the staff. Therefore, the objective of EVSR is essentially to achieve a good trade-off between the investment cost and the operation cost. In the numerical experiments in Section 5, we further develop specific case studies to quantitatively analyze the relationship between these two objectives.

3.3.3. Mathematical model

According to the above descriptions, the optimization model for EVSR can be formulated as a mixed-integer linear programming (MILP) model, given as follows:

$$\min \quad c^a\sum_{i\in\mathbf{I}} H_i + c^y\sum_{i\in\mathbf{I}} F_i + \sum_{h\in\mathbf{H}}\sum_{(i,t,j,s)\in\mathbf{A}} c^l_{ij}X^h_{it\,js} + \sum_{(i,t,j,s)\in\mathbf{A}} c^d_{ij}\Big(\sum_{f\in\mathbf{F}} Z^f_{it\,js} - \sum_{h\in\mathbf{H}} X^h_{it\,js} + N_{it\,js}\Big), \tag{17}$$

$$\text{s.t.}\begin{cases} (1)-(9),\ (11)-(14) \\ X^h_{ijts},\ Z^f_{ijts}\in\{0,1\}, \quad \forall (i,t,j,s)\in\mathbf{A},\ h\in\mathbf{H},\ f\in\mathbf{F}, & (18)\\ E^h_t\in\mathbb{N}, \quad \forall h\in\mathbf{H},\ t\in\mathbf{T}, & (19)\\ H_i,\ F_i\in\mathbb{N}, \quad \forall i\in\mathbf{I}. & (20)\end{cases}$$

Remark 3.4. Note that the proposed EVSR model actually provides a typical framework for the strategic planning problems in one-way carsharing systems. By slightly adjusting the objective function or certain constraints, it can be easily generalized into different versions according to the specific requirement of carsharing company. For example, if the urban area has very limited EV parking capacity, we can add the following set of constraints into the original model to handle the cases with station capacity, i.e.,

$$\sum_{h\in\mathbf{H}}\sum_{(j,s)\in\mathbf{V}:(i,t,j,s)\in\mathbf{A}} X^h_{it\,js} \le C_i, \qquad \forall (i,t)\in\mathbf{V} \tag{21}$$

where C_i is the capacity of each station $i\in\mathbf{I}$. Even though, we still note that adding this set of constraints would also make the model even harder to be solved (See the numerical experiments in Appendix A). As we assume that the one-way chasharing is well designed that the station capacities are sufficient to serve the user reservations, we will address to solve the uncapacitated EVSR problem in the following content. On the other hand, we can also transform the original service-driven model that aims to serve all the reservations into a pure profit-driven model that maximizes the total system profits by relaxing the user fulfilling constraints and adding the part of system revenue to the objective function. In practice, the operator can choose either of these models with respect to different requirements of carsharing company.

4. Lagrangian relaxation-based solution approach

The formulated MILP model in Section 3.3.3 is essentially a variation of the vehicle routing problem (VRP), which is apparently NP-hard problem (see Min (1989); Hosni et al. (2014); Toth and Vigo (2014) and Mahmoudi and Zhou (2016)). Different from traditional VRP, the proposed model contains several sets of additional hard constraints, e.g., constraints (5), (6), (12)–(14). Therefore, it is significantly more challenging to solve the proposed model. We first try to solve this problem with commercial solvers including CPLEX and Gurobi, but we find that they have difficulty in solving even medium-scale instances (see the experiments in Section 5.1 for details) in a reasonable time. To tackle this computational challenge, we particularly propose a customized solution approach based on the Lagrangian relaxation embedded with dynamic programming (DP) and greedy algorithm, in order to solve the model to optimum (or near-optimum) in a much shorter time.

In the following content, Section 4.1 proposes a Lagrangian relaxation-based decomposition approach to obtain the lower bound of the optimal value of objective function (17). Specifically, by relaxing the coupling hard constraints (5) and (6), we

decompose the primal problem into a series of sub-problems that can be regarded as several RCSP problems, SP problems and SA problems, which can be solved efficiently to the optimum by exact algorithms in the space-time network. However, the relaxed solution is likely infeasible to the original problem. Hence, a three-phase implementing algorithm is further developed to adjust the solution of the relaxed model into a feasible solution to the primal problem according to the values of Lagrangian multipliers. Furthermore, Section 4.3 adopts a subgradient algorithm to iteratively update the upper and lower bounds to obtain a near-optimal solution.

4.1. Model decomposition

First, we note that, the EV space-time traveling indicators $\mathbf{X} := \{X^h_{it\,js}\}_{(i,t,j,s)\in\mathbf{A},h\in\mathbf{H}}$ do not specify if each vehicle h is operated by a staff member or a user, which makes it difficult to decompose the primal problem. To this end, we here introduce new EV space-time arc variables $\mathbf{Y} := \{Y^h_{it\,js}\}_{(i,t,j,s)\in\mathbf{A},h\in\mathbf{H}}$ as a set of "user flag" indicators to determine if assigning the EVs to corresponding user reservations. Specifically, we define $Y^h_{it\,js} = 1$ if vehicle h is picked up by a user from parking station i at time t, and dropped to parking station j at time s; and $Y^h_{it\,js} = 0$ otherwise. Then, constraints (5) are equivalently substituted by the following constraints:

$$X^h_{it\,js} \geq Y^h_{it\,js}, \quad \forall (i,t,j,s) \in \mathbf{A}, \quad h \in \mathbf{H}, \tag{22}$$

$$\sum_{h\in\mathbf{H}} Y^h_{it\,js} = N_{it\,js}, \quad \forall (i,t,j,s) \in \mathbf{A}, \tag{23}$$

$$Y^h_{it\,js} \in \{0,1\}, \quad \forall (i,t,j,s) \in \mathbf{A}, \quad h \in \mathbf{H}. \tag{24}$$

Constraints (22) indicate the relationship between variables **X** and **Y**. Constraints (23) ensure that all user reservations are fulfilled. Constraints (24) enforce the binary constraints. It is clear that the reformulated model is actually equivalently to the origin model. Note that another feasible way to represent the vehicle to passenger assignment is to define the demand on each space-time arc, which requires the "variable-splitting" technique for solution symmetry breaking. We can refer to Fisher et al. (1997); Kohl et al. (1999); Tong et al. (2017) and Niu et al. (2018) for more details.

Then, we see from the primal problem that constraints (6) and (22) are hard coupling constraints. In particular, Constraints (6) connect EV rebalancing and staff relocation process, while constraints (22) postulate relationships between traveling arcs of EVs and users. Thus, we relax these two sets of constraints and add them to objective function (17) by introducing two sets of Lagrangian multipliers $\boldsymbol{\lambda} := \{\lambda_{itjs} \geq 0\}_{(itjs)\in\mathbf{A}}$ and $\boldsymbol{\mu} := \{\mu^h_{it\,js} \geq 0\}_{(it\,js)\in\mathbf{A},h\in\mathbf{H}}$, respectively. In this way, the primal problem can be relaxed into the following formulations:

$$\begin{aligned}\Delta(\boldsymbol{\lambda},\boldsymbol{\mu}) := \min_{\mathbf{X},\mathbf{Y},\mathbf{Z}} \; & c^a \sum_{i\in\mathbf{I}} H_i + c^y \sum_{i\in\mathbf{I}} F_i + \sum_{(i,t,j,s)\in\mathbf{A}} \sum_{h\in\mathbf{H}} (c^l_{ij} - c^d_{ij} + \lambda_{it\,js} - \mu^h_{it\,js}) X^h_{it\,js} \\ & + \sum_{(i,t,j,s)\in\mathbf{A}} \sum_{f\in\mathbf{F}} (c^d_{ij} - \lambda_{it\,js}) Z^f_{it\,js} + \sum_{(i,t,j,s)\in\mathbf{A}} \sum_{h\in\mathbf{H}} \mu^h_{it\,js} Y^h_{it\,js} + \sum_{(i,t,j,s)\in\mathbf{A}} (c^d_{ij} - \lambda_{it\,js}) N_{it\,js}\end{aligned} \tag{25}$$

subject to constraints (1)–(4), (7)–(9), (11)–(14), (18)–(20), (23) and (24).

Note that since the coupling constraints (6) and (22) are relaxed, variables **X, Z** and **Y** are separated from each other in the relaxed problem, which can be finally decomposed into three sets of sub-problems as follows.

Remark 4.1. Note that direct relaxation of constraints (5) will lead to an excessive looseness of primary problem and poor performance of LR relaxation algorithm since the variables **X** and **Z** are not linked to each specific user activity. In contrast, we first introduce the user flag variables **Y** to explicitly indicate the assignment of user activities to each EV. This kind of treatment can provide a good connection between the LR multipliers and feasible solutions after the relaxation of new constraints (22), and thus captures the gap variation between the upper and lower bound during the Lagrangian multiplier updating process. Essentially, by employing "variable-splitting" technique, the primal problem is essentially divided into three sub-problems that respectively determine the EV routing, staff dispatching and EV-user assignment plans, and multipliers $\boldsymbol{\lambda}$ and $\boldsymbol{\mu}$ serve as the mediator among these three sub-problems.

Subproblem 1: Resource constrained shortest path problems

The first set of subproblems includes $|\mathbf{H}|$ subproblems, each of which can be seen as a RCSP problem with one vehicle $h \in \mathbf{H}$, as follows:

$$\Gamma_h(\boldsymbol{\lambda},\boldsymbol{\mu}) := \min_{\mathbf{X}} \; c^a \sum_{i\in\mathbf{I}} X^h_{i_0 t_0 i t_0} + \sum_{(i,t,j,s)\in\mathbf{A}} (c^l_{ij} - c^d_{ij} + \lambda_{it\,js} - \mu^h_{it\,js}) X^h_{it\,js}, \tag{26}$$

subject to (1), (3), (9), (11)–(14), (18)–(20).

We can see that objective function (26) is composed of two parts. The first part is the amortized cost that is fixed for each given vehicle $h \in \mathbf{H}$. The second part is the generalized traveling cost related to the routing paths of the EVs in the constructed space-time network. Thus the optimization of this part can be seen as a time-dependent least-cost routing

path problem that can be solved to the optimum by some exact solution approaches (e.g., label correcting (Yang and Zhou, 2014; 2017) and DP (Mahmoudi and Zhou, 2016)). We define $\eta^h_{it\,js} := c^l_{ij} - c^d_{ij} + \lambda_{it\,js} - \mu^h_{it\,js}$ to denote the generalized cost of vehicle h when traveling through space-time arc $(i, t, j, s) \in \mathbf{A}$.

Furthermore, to capture the EV battery charging and consumption dynamics, we extend the space-time network by adding the charge-status dimension of battery levels as typically done in the studies where resource-space-time network is utilized (Erdogan and Miller-Hooks, 2012; Schneider et al., 2014; Lu et al., 2016; Mahmoudi and Zhou, 2016). We initially discretize the battery volume as a set of battery level indexes $\mathbf{R} = \{0, \sigma, 2\sigma, \cdots, E_0\}$ (indexed by r), where σ denotes the battery volume between each two adjacent battery level. Note that the value of σ shall be properly given based on the value of E_0, E^+, and E^-. Then we introduce the parameter L^h_{itr} to denote the traveling cost state of h at space-time vertex (i, t) with the battery level of r. Specifically, we assume that the initial battery levels of all the EVs share the same value of E_0. We here define the travel time between stations i and j as T_{ij}. Then the arrival time s of each space-time arc $(i, t, j, s) \in \mathbf{A}$ can be derived by given the departure time t and T_{ij} as $s = t + T_{ij}$. The parameter ΔE_{ij} is adopted to denote the variation of battery level when EVs traveling between parking station i and j. Specifically, we have $\Delta E_{ii} = E^+, \ \forall i \in \mathbf{I}$ to denote the charging quantity when EVs dwell in parking station i for each time interval, while $\Delta E_{ij} = T_{ij}E^-$ to represent the consumption quantity when EVs travel between parking stations i and j ($\forall i, j \in \mathbf{I}, i \neq j$). Eventually, an optimal solution approach based on DP for the RCSP problems is developed, which is described in Algorithm 1, and the time complexity of solving all $|\mathbf{H}|$

Algorithm 1 An optimal solution approach for solving sub-problem $\Gamma_h(\boldsymbol{\lambda}, \boldsymbol{\mu})$.

Step 1. Initialize:

(a) $L^h_{itr} = M, \quad \forall (i,t) \in \mathbf{V}, \ r \in \mathbf{R}, \ h \in \mathbf{H}$ to denote the traveling cost state of vehicle h at space-time vertex (i,t) with battery level of r, where M is a very large positive value;

(b) $PN^h_{itr} = 0$, $PT^h_{itr} = 0$, and $PR^h_{itr} = 0, \quad \forall (i,t) \in \mathbf{V}, \ r \in \mathbf{R}, \ h \in \mathbf{H}$ to record the previous station, time and battery level of space-time vertex (i,t) with battery level of r in the least-cost routing path of vehicle h, respectively;

(c) Set $\mathbf{P}_h = \varnothing, \quad \forall h \in \mathbf{H}$ to record the space-time arcs within the least-cost routing path of vehicle h;

Step 2. Do for each vehicle $h \in \mathbf{H}$;

Step 2.1 Set $L^h_{i_O t_O E_0} = 0$;

Step 2.2 Do for each space-time arc $(i, t, j, s) \in \mathbf{A}$;Do for each battery level r:

If $r + \Delta E_{ij} > 0$, then make the following judgments:

(a) If $r + \Delta E_{ij} > E_0$, then $r' = E_0$; and $r' = r + \Delta E_{ij}$ otherwise;

(b) If $L^h_{itr} + \eta^h_{it\,js} < L^h_{jsr'}$, update the traveling cost state as $L^h_{jsr'} = L^h_{itr} + \eta^h_{it\,js}$, and update the previous station, time and battery level of space-time arc (j,s) with battery level r' as $PN^h_{jsr'} = i$, $PT^h_{jsr'} = t$ and $PR^h_{jsr'} = r$;

Step 2.3 Select $L^h_{i^*(t_0+M\delta)r^*} = \min\{L^h_{i(t_0+M\delta)r}\}_{i\in\mathbf{I}, r\in\mathbf{R}}$;

Step 2.4 If $L^h_{i^*(t_0+M\delta)r^*} + c^a < 0$, track back from space-time vertex $(i^*, t_0 + M\delta)$ with battery level of r^* to dummy origin vertex (i_O, t_O) using the values of PN^h_{itr}, PT^h_{itr}, and PR^h_{itr}, and record all the relative space-time arcs in set $\mathbf{P}_h$;

Step 3. Return set $\mathbf{P}_h, \quad \forall h \in \mathbf{H}$, then the relaxed solution of $\mathbf{X}$ can be obtained as:

$$\hat{X}^h_{it\,js} = \begin{cases} 1 & \text{if } (i,t,j,s) \in \mathbf{P}_h, \\ 0 & \text{otherwise,} \end{cases} \quad \forall h \in \mathbf{H};$$

Step 4. Return the optimal solution $\{\hat{X}^h_{it\,js}\}_{h\in\mathbf{H},(i,t,j,s)\in\mathbf{A}}$ of relaxed model and the objective function value $\Gamma_h(\boldsymbol{\lambda}, \boldsymbol{\mu})$.

sub-problems (26) is at most $O(|\mathbf{H}|(|\mathbf{I}|^2 + 1)|\mathbf{T}||\mathbf{R}|)$.

Subproblem 2: Shortest path problems

Similarly, subproblem 2 contains $|\mathbf{F}|$ sub-problems, each of which can be seen as a SP problem associated with one staff member $f \in \mathbf{F}$:

$$\Pi_f(\boldsymbol{\lambda}) := \min_{\mathbf{Z}} \quad c^y \sum_{i\in\mathbf{I}} Z^f_{i_O t_O i t_O} + \sum_{(i,t,j,s)\in\mathbf{A}} (c^d_{ij} - \lambda_{it\,js}) Z^f_{it\,js}, \tag{27}$$

subject to constraints (2), (7), (18) and (20).

Note that object function (27) has a similar structure as (26) by mapping the vehicle amortized cost c^a and generalized vehicle traveling cost $\eta^h_{it\,js}$ to the staff hiring cost c^y and generalized staff traveling cost $\xi_{it\,js} = c^d_{ij} - \lambda_{it\,js}$, respectively. Differently, we note that since the generalized staff traveling cost ξ_{itjs} is constant for different staff members, all the staff will share the same least-cost routing path as an optimal solution to problem (27). Besides, since battery charging related constrains are not concerned for staff traveling paths, sub-problem (27) is essentially a set of SP problems that is much less complicated. Therefore, we also adopt a DP-based algorithm, which is described in Algorithm 2 that takes a time complexity of no more than $O((|\mathbf{I}|^2 + 1)|\mathbf{T}|)$.

Subproblem 3: Semi-assignment problem

Algorithm 2 An optimal solution approach for solving sub-problem $\Pi_f(\boldsymbol{\lambda})$.

Step 1. Initialize:
(a) $L_{it} = M, \quad \forall (i,t) \in \mathbf{V}$ as the staff traveling cost state at space-time vertex (i,t) and set $L_{i_0 t_0} = 0$ specially;
(b) $PN_{it} = 0$ and $PT_{it} = 0, \quad \forall (i,t) \in \mathbf{V}$ to record the previous station and time of space-time vertex (i,t) in the common least-cost routing path of staff, respectively;
(c) Set $\mathbf{P} = \varnothing$ to record the space-time arcs in the common least-cost routing path of staff;
Step 2. Do for each space-time arc $(i,t,j,s) \in \mathbf{A}$;
Step 2.1 If $L_{it} + \xi_{itjs} < L_{js}$, update the traveling cost state as $L_{js} = L_{it} + \xi_{itjs}$, and the previous parking station and time of space-time vertex (j,s) as $PN_{js} = i$ and $PT_{js} = t$;
Step 3. Select $L_{i^*(t_0+M\delta)} = \min\{L_{i(t_0+M\delta)}\}_{i\in\mathbf{I}}$;
Step 4. If $L_{i^*(t_0+M\delta)} + c^y < 0$, track back from space-time vertex $(i^*, t_0 + M\delta)$ to dummy origin vertex (i_0, t_0) using the values of PN_{it} and PT_{it}, and record all the relative space-time arcs in set $\mathbf{P}$;
Step 5. Return set $\mathbf{P}$, then the relaxed solution of $\mathbf{Z}$ can be obtained as:

$$\hat{Z}^f_{itjs} = \begin{cases} 1 & \text{if } (i,t,j,s) \in \mathbf{P}, \\ 0 & \text{otherwise}, \end{cases} \quad \forall (i,t,j,s) \in \mathbf{A}, f \in \mathbf{F};$$

Step 5. Return the relaxed solution $\{\hat{Z}^f_{itjs}\}_{f\in\mathbf{F},(i,t,j,s)\in\mathbf{A}}$ and the objective function value $\Pi_f(\boldsymbol{\lambda})$.

The subproblem 3 only includes one sub-problem with respect to variables $\mathbf{Y}$, given as follows

$$\Phi(\boldsymbol{\lambda}, \boldsymbol{\mu}) := \min_{\mathbf{Y}} \sum_{(i,t,j,s)\in\mathbf{A}} \sum_{h\in\mathbf{H}} \mu^h_{itjs} Y^h_{itjs} + \sum_{(i,t,j,s)\in\mathbf{A}} (c^d_{ij} - \lambda_{itjs}) N_{itjs}, \tag{28}$$

subject to constraints (23) and (24).

The structure of subproblem 3 is very simple that the exact optimal solution can be easily obtained as follows. For each space-time arc $(i,t,j,s) \in \mathbf{A}_u$, where $\mathbf{A}_u = \{(i,t,j,s) \in \mathbf{A} | N_{itjs} \neq 0\}$, we define the set $\mathbf{H}^*_{itjs} = \{h^{(1)}, h^{(2)}, \cdots, h^{(N_{itjs})}\}$ to denote the first N_{itjs} vehicles sorted by the values of their corresponding Lagrangian multipliers, i.e., $\mu^{h^{(k)}}_{itjs} < \mu^{h'}_{itjs}$, where $1 \le k \le N_{itjs}$, $k \in \mathbb{Z}^+$ and $h' \in \mathbf{H} \backslash \mathbf{H}^*_{itjs}$. In other words, we first sort the set of Lagrangian multipliers μ^h_{itjs} for all the $h \in \mathbf{H}$ from the smallest to the largest. Then, we pick the smallest N_{itjs} multipliers and let the corresponding Y^h_{itjs} equal to 1. Repeat the process above for all the space-time arcs $(i,t,j,s) \in \mathbf{A}_u$, and the optimal solution to sub-problem 3 (denoted by $\hat{\mathbf{Y}} := \{\hat{Y}^h_{itjs}\}_{(itjs)\in\mathbf{A},h\in\mathbf{H}}$) can be represented as:

$$\hat{Y}^h_{itjs} = \begin{cases} 1 & \text{if } h \in \mathbf{H}^*_{itjs}, \\ 0 & \text{otherwise}, \end{cases} \quad \forall (i,t,j,s) \in \mathbf{A}, \ \forall h \in \mathbf{H}. \tag{29}$$

Proposition 1. *Equation (29) yields the optimal solution to model (28).*

Proof. See Appendix B. □

Note that subproblem 3 essentially optimizes the assignment plan between EVs and user reservations based on the values of Lagrangian multipliers μ. That is, the vehicles with smaller μ will be dispatched to satisfy the reservations. And the corresponding algorithm, which only takes a time complexity of $O(|\mathbf{A_u}||\mathbf{H}|ln(|\mathbf{H}|))$ (see Li (2013)), is very efficient and also employed in Fisher et al. (1997) for solving semi-assignment problem.

After solving the sub-problems (26)–(28) with relaxed solution of **X, Y** and **Z**, the optimal objective value to relaxed problem (25) for a set of given $\boldsymbol{\lambda}$ and $\boldsymbol{\mu}$ can be obtained by:

$$\Delta(\boldsymbol{\lambda}, \boldsymbol{\mu}) = \sum_{h\in\mathbf{H}} \Gamma_h(\boldsymbol{\lambda}, \boldsymbol{\mu}) + \sum_{f\in\mathbf{F}} \Pi_f(\boldsymbol{\lambda}) + \Phi(\boldsymbol{\lambda}, \boldsymbol{\mu}), \tag{30}$$

which also serves as the lower bound to the optimal value of the primal problem according to the duality property of Lagrangian relaxation (see Geoffrion (1974)).

4.2. Dynamic programming based implementing algorithms

If the relaxed solutions (denoted by $\hat{\mathbf{X}} := \{\hat{X}^h_{itjs}\}_{h\in\mathbf{H},(i,t,j,s)\in\mathbf{A}}$ and $\hat{\mathbf{Z}} := \{\hat{Z}^f_{itjs}\}_{f\in\mathbf{F},(i,t,j,s)\in\mathbf{A}}$) obtained by solving sub-problems 1 and 2 are found to be feasible to the primal problem, then they are also the optimal solutions to the primal problem. Otherwise, we need to develop some heuristics to modify the relaxed solution into a feasible one (denoted by $\bar{\mathbf{X}} := \{\bar{X}^h_{itjs}\}_{h\in\mathbf{H},(i,t,j,s)\in\mathbf{A}}$ and $\bar{\mathbf{Z}} := \{\bar{Z}^f_{itjs}\}_{f\in\mathbf{F},(i,t,j,s)\in\mathbf{A}}$), which is a typical method adopted by many previous studies e.g., see Li and Ouyang (2012); Hosni et al. (2014); Diabat et al. (2015); Fu and Diabat (2015); An and Ouyang (2016); Bai et al. (2016); Liu and Zhou (2016) and Yang and Zhou (2017).

Even though the values of $\hat{\mathbf{Y}}$ are subject to constraints (23), i.e., the user demand fulfilling constraints, the optimal solution of the relaxed problem may be still infeasible since space-time flow balance constraints (3) are not taken into consideration. An illustrative example is shown in Fig. 4 (a), where we consider that four reserved trips (shown as blue dashed arrows) are assigned to one vehicle h_1 based on the value of $\{\hat{Y}^{h_1}_{it\,js}\}$ (i.e., the optimal solution to the relaxed model). Nevertheless, it can be clearly seen that only part of these four reservations can be accomplished by vehicle h_1 according to the space-time flow balance constraints. In this case, the four reservations have to be reassign to at least two EVs. To overcome this problem, a three-phase implementing algorithm, which involves screening procedure, EV reassigning procedure and staff dispatching procedure, is particularly developed to reassign the user reservations to EVs and then generate the corresponding staff dispatching paths to perform the relocation tasks.

Phase 1: Screening procedure

First, we screen the task schedule of h_1 and remove the reservations that cannot be practically satisfied, which is termed as screening procedure. A dynamic programming based greedy (DPG) algorithm is adopted here to adjust the previous routing plan to cover as many reserved trips as possible with the least traveling cost (shown as black solid arrows in Fig. 4 (a)). In specific, we generate the generalized traveling cost for h_1 by setting the space-time arcs of these four reserved trips with negative cost $-M$ and others with positive cost c^l_{ij} for any $(i, j)\in\mathbf{L}$, where M is a very large positive value. In this constructed network, the shortest path of vehicle h_1 by DPG algorithm can obviously cover as many reserved trips as possible with the least traveling cost.

Phase 2: EV reassigning procedure

Then, we reassign the remaining reservations that are removed from the schedule of h_1 to other EVs. Particularly, for the remaining reserved trips $(1, t_0+\delta, 2, t_0+3\delta)$ and $(1, t_0+5\delta, 2, t_0+7\delta)$, we dispatch a spare EV h_2, which satisfies $\sum_{(it\,js)\in\mathbf{A}}\hat{Y}^{h_2}_{it\,js}=0$, to cover as many trips as possible with the least traveling cost, and similarly, the routing plan of h_2 is also generated by the DPG algorithm (shown as black dashed arrows in Fig. 4 (b)). In this way, this process will be repeated for all the other spare EVs until all the user trips are fully covered. In detail, the consolidated process of screening and EV reassigning procedures are presented in Algorithm 3, which returns a feasible solution of EV dispatching strategy. The time complexity of this algorithm is no more than $O(|\mathbf{H}|(|\mathbf{I}|^2+1)|\mathbf{T}||\mathbf{R}|)$.

Phase 3: Staff dispatching procedure

Based on the feasible solution $\bar{\mathbf{X}}$ obtained from Algorithm 3, we further perform the staff dispatching procedure in order to generate the feasible staff relocation plan obtained from $\bar{\mathbf{Z}}$. In specific, we first calculate the number of EV rebalancing trips that should be accomplished by staff on each space-time arc (denoted by l_{itjs}, $\forall(i, t, j, s)\in\mathbf{A}$) as follows:

$$l_{it\,js}=\begin{cases}\sum_{h\in\mathbf{H}}\bar{X}^h_{it\,js}-N_{it\,js} & \text{if } i\neq j\vee(i,t)\neq(i_O,t_O)\vee(i,t)\neq(i_D,t_D),\\ 0 & \text{otherwise.}\end{cases}$$

If $l_{itjs}>0$, we set the corresponding staff traveling cost as $\gamma^f_{it\,js}=-M$; otherwise, we set $\gamma^f_{it\,js}=c^d_{ij}$. Then, the DPG algorithm above is called repeatedly to make routing schedules, each of which covers as many rebalancing trips as possible with the least traveling cost. The process will be terminated until all the EV rebalancing trips are fully covered by the involved staff. As shown in Fig. 4 (c) , with the given $\bar{\mathbf{X}}$, there are two rebalancing trips that need to be covered, which are denoted by space-time arcs $(2, t_0+2\delta, 3, t_0+3\delta)$ and $(2, t_0+3\delta, 1, t_0+5\delta)$, respectively. Using the process above, we know that, two staff members, i.e., f_1 and f_2, are involved to accomplish the rebalancing tasks and the routing plan is shown as red solid and red dashed arrows, respectively. In particular, the staff dispatching procedure is presented as Algorithm 4 that takes a time complexity of no more than $O(|\mathbf{F}|(|\mathbf{I}|^2+1)|\mathbf{T}|)$.

Eventually, the feasible objective value is obtained by plugging the value of $\bar{\mathbf{X}}$ and $\bar{\mathbf{Z}}$ into primal objective function (17), which serves as the upper bound of the EVSR model.

4.3. Updating Lagrangian multipliers

If the upper bound obtained in Section 4.2 is happened to be equal to the lower bound (30), we can return the corresponding feasible solution, which is guaranteed to be the optimal solution according to the duality theory (Fisher, 1981). Otherwise, we need to iteratively update the values of multipliers $\boldsymbol{\lambda}$ and $\boldsymbol{\mu}$ to obtain a tighter gap between the current relaxed and feasible solution, which will potentially improve the feasible solution. Therefore, we adopt a standard subgradient algorithm to execute the iteration process. The subgradient algorithm is a widely used approach for updating Lagrangian multipliers (see Li (2013); An et al. (2015); Ouyang et al. (2015); Cui et al. (2016); Yin et al. (2017)), and we briefly describe its main procedure for the completeness of this paper.

In this study, we first give a set of initial Lagrangian multipliers $\{(\lambda_{it\,js})^{k=0}\}_{(it\,js)\in\mathbf{A}}$ and $\{(\mu^h_{it\,js})^{k=0}\}_{(it\,js)\in\mathbf{A},h\in\mathbf{H}}$ with values of 0, in which k represents the number of iterations. By using the subgradient algorithm, Lagrangian multipliers $(\lambda_{itjs})^k$ and $(\mu^h_{it\,js})^k$ are updated to $(\lambda_{it\,js})^{k+1}$ and $(\mu^h_{it\,js})^{k+1}$ by

$$(\lambda_{it\,js})^{k+1}=\max\{0,\,(\lambda_{it\,js})^k+t_k(\sum_{h\in\mathbf{H}}(\hat{X}^h_{it\,js})^k-\sum_{f\in\mathbf{F}}(\hat{Z}^f_{it\,js})^k-N_{it\,js})\},\tag{31}$$

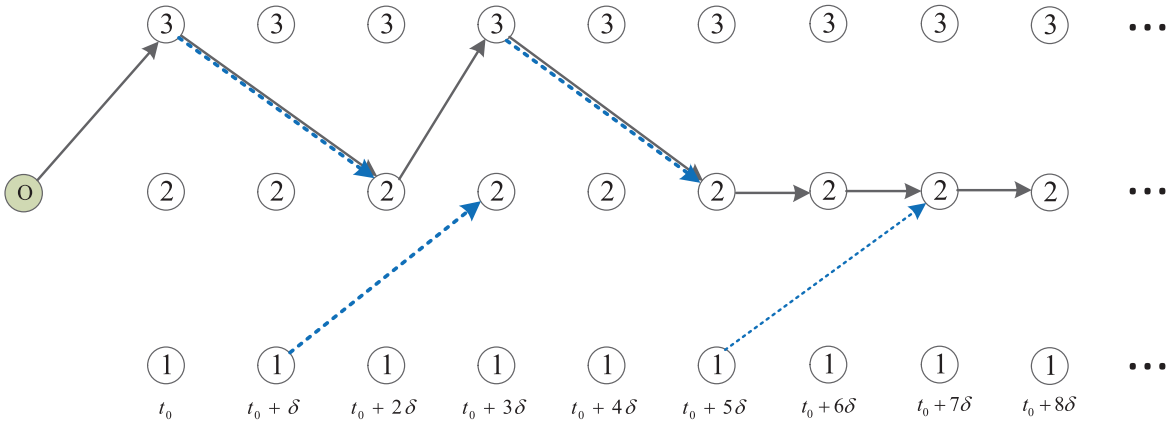

(a) Screening procedure of implementing algorithm

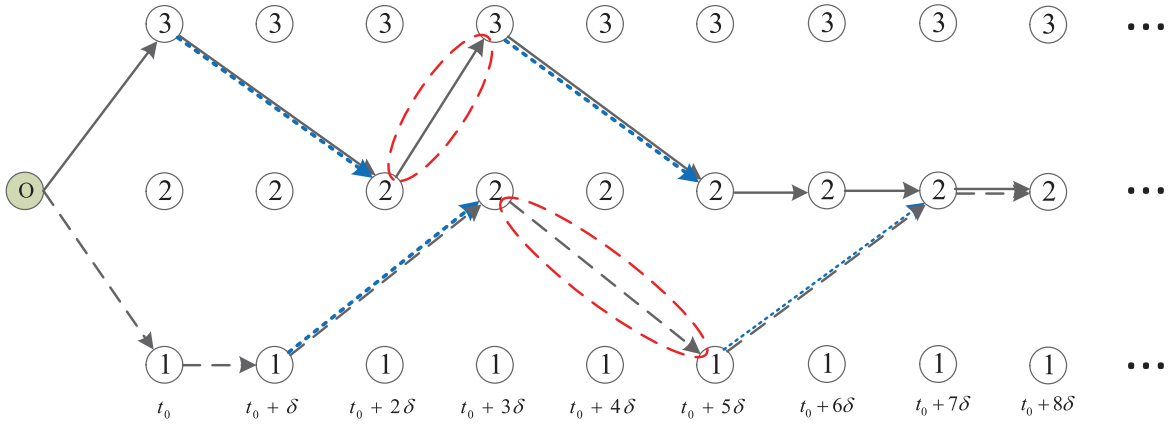

(b) EV reassigning procedure of implementing algorithm

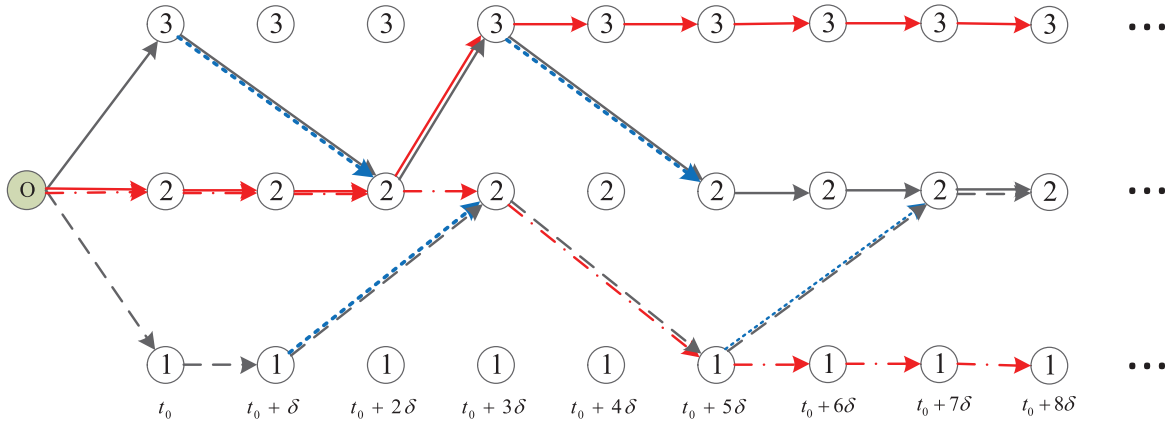

(c) Staff dispatching procedure of implementing algorithm

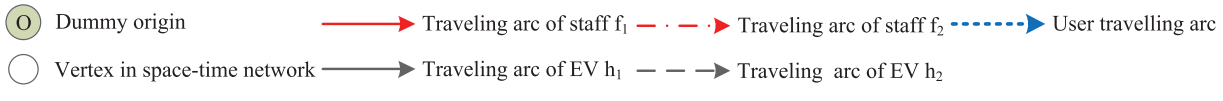

Fig. 4. Illustration for three-phase implementing algorithm.

Algorithm 3 Screening and EV reassigning procedure for constructing feasible paths of EVs by DP.

Step 1. Initialize:

(a)$L^h_{itr} = M, \quad \forall (i,t) \in \mathbf{V}, \ r \in \mathbf{R}, \ h \in \mathbf{H}$ as the traveling cost state of vehicle h at space-time vertex (i,t) with battery level of r;

(b) Set $PN^h_{itr} = 0$, $PT^h_{itr} = 0$, and $PR^h_{itr} = 0, \quad \forall (i,t) \in \mathbf{V}, \ r \in \mathbf{R}, \ h \in \mathbf{H}$ to record the previous station, time and battery level of space-time vertex (i,t) with battery level of r in the least-cost routing path of vehicle h, respectively;

(c) Set $\mathbf{P}_h = \varnothing, \quad \forall h \in \mathbf{H}$ to record the space-time arcs within the least-cost routing path of vehicle h;

(d) Set $\overline{\mathbf{H}} = \{h | \sum_{(i,t,j,s)\in\mathbf{A}} \hat{Y}^h_{itjs} > 0\} \subseteq \mathbf{H}$, and then generate the generalized vehicle traveling cost for each EV $h \in \overline{\mathbf{H}}$ on each space-time arc (i,t,j,s) (denoted by ρ^h_{itjs}) as:

$$\rho^h_{itjs} = \begin{cases} -M & \text{if } \hat{Y}^h_{itjs} = 1, \\ c^l_{ij} & \text{otherwise;} \end{cases} \quad \forall h \in \overline{\mathbf{H}}, \ (i,t,j,s) \in \mathbf{A};$$

(e) Define task counting variable k_{itjs} for $\forall (i,t,j,s) \in \mathbf{A}$ to record the number of user trips that are not fulfilled on space-time arc (i,t,j,s);

Step 2. (Screening procedure) Do for each vehicle $h \in \overline{\mathbf{H}}$:

Step 2.1. Call Step 2.1–2.4 of Algorithm 1 (map η^h_{itjs} to ρ^h_{itjs}) and return $\mathbf{P}_h$;

Step 2.2. Do for each space-time arc $(i,t,j,s) \in \mathbf{A} \backslash \mathbf{P}_h$:

If $\hat{Y}^h_{itjs} = 1$, update $k_{itjs} = k_{itjs} + 1$;

Step 3. (Reassignment procedure) If $k_{itjs} = 0, \forall (i,t,j,s) \in \mathbf{A}$, then turn to Step 4; otherwise, do for another vehicle $h \in \mathbf{H} \backslash \overline{\mathbf{H}}$;

Step 3.1. Generate the generalized vehicle traveling cost of vehicle h on each space-time arc (i,t,j,s) (denoted by θ^h_{itjs}) as:

$$\theta^h_{itjs} = \begin{cases} -M & \text{if } k_{itjs} > 0, \\ c^l_{ij} & \text{otherwise;} \end{cases} \quad \forall (i,t,j,s) \in \mathbf{A};$$

Step 3.2. Call Step 2.1–2.4 of Algorithm 1 (map η^h_{itjs} to θ^h_{itjs}) and return $\mathbf{P}_h$;

Step 3.3. Do for each space-time arc $(i,t,j,s) \in \mathbf{P}_h$:

If $k_{itjs} > 0$, update $k_{itjs} = k_{itjs} - 1$;

Step 3.4. Update $\overline{\mathbf{H}} = \overline{\mathbf{H}} \cup \{h\}$ and repeat Step 3;

Step 4. Obtain the feasible solution $\bar{\mathbf{X}}$ as:

$$\bar{X}^h_{itjs} = \begin{cases} 1 & \text{if } (i,t,j,s) \in \mathbf{P}_h, \\ 0 & \text{otherwise,} \end{cases} \quad \forall (i,t,j,s) \in \mathbf{A}, h \in \mathbf{H};$$

Step 5. Return the feasible solution $\bar{\mathbf{X}}$.

and

$$(\mu^h_{itjs})^{k+1} = \max\{0, (\mu^h_{itjs})^k + t_k((\hat{Y}^h_{itjs})^k - (\hat{X}^h_{itjs})^k)\}, \tag{32}$$

in which $\hat{\mathbf{X}}^k$, $\hat{\mathbf{Y}}^k$ and $\hat{\mathbf{Z}}^k$ are the optimal solutions of relaxed models in the kth iteration, and t_k is the step size that is computed in each iteration by

$$t_k = \frac{\tau^k (UB^k - LB^k(\boldsymbol{\lambda}, \boldsymbol{\mu}))}{\sum_{(i,t,j,s)\in\mathbf{A}} \left(\left(\sum_{h\in\mathbf{H}} (\hat{X}^h_{itjs})^k - \sum_{f\in\mathbf{F}} (\hat{Z}^f_{itjs})^k - N_{itjs} \right)^2 + \sum_{h\in\mathbf{H}} \left((\hat{Y}^h_{itjs})^k - (\hat{X}^h_{itjs})^k \right)^2 \right)} \tag{33}$$

where UB^k and $LB^k(\boldsymbol{\lambda}, \boldsymbol{\mu})$ are the best upper bound and lower bound up to iteration k, and τ^k is the step parameter in the subgradient algorithm. In our study, we note that, if the lower bound does not improve in K_c iterations (set as 10 in our experiments), then we update this parameter as $\tau^{k+1} \leftarrow \tau^k/\theta$, where θ represents the contraction ratio that is greater than 1.

Based on the introduction of Lagrangian relaxation scheme, developed DPG algorithm and the Lagrangian multiplier updating methods, we summarize the general procedure of Lagrangian relaxation based (LR) algorithm process in Algorithm 5.

5. Numerical examples

In Section 5.1, we first derive a set of relatively small-scale numerical experiments to verify the effectiveness of the proposed model and algorithms. In particular, we compare the performance of our solution approach with two commonly used commercial solvers: CPLEX and Gurobi. Then, based on the real-world case of Seattle one-way carsharing system, we illustrate and analyze the EVSR strategies that are obtained by our developed solution approach in Section 5.2, where we also

Algorithm 4 Staff dispatching procedure for constructing feasible paths of staff members by DP.

Step 1. Initialize:

(a) $L_{it}^{f} = M, \quad \forall (i,t) \in \mathbf{V}, \quad f \in \mathbf{F}$ as the traveling cost state of staff member f at space-time vertex (i,t);

(b) $PN_{it}^{f} = 0$ and $PT_{it}^{f} = 0, \quad \forall (i,t) \in \mathbf{V}, \quad f \in \mathbf{F}$ to record the previous station and time of each space-time vertex (i,t) in the routing path of staff member f, respectively;

(c) Sets $\mathbf{P}_f = \varnothing, \quad \forall f \in \mathbf{F}$ to record the space-time arcs within the least-cost routing path of staff member f;

(d) Set $\bar{\mathbf{F}} = \mathbf{F}$ to record the staff that are not sent out;

(e)

$$l_{it\,js} = \begin{cases} \sum_{h \in \mathbf{H}} \bar{X}_{it\,js}^{h} - N_{it\,js} & \text{if } i \neq j \vee (i,t) \neq (i_O, t_O) \vee (i,t) \neq (i_D, t_D), \\ 0 & \text{otherwise}, \end{cases}$$

to record the number of rebalancing trips for staff on each space-time arc;

Step 2. If $l_{it\,js} = 0, \quad \forall (i,t,j,s) \in \mathbf{A}$, then turn to Step 3; Otherwise, Do for one $f \in \bar{\mathbf{F}}$:

Step 2.1. Generate the generalized vehicle traveling cost on each space-time arc (denoted by $\gamma_{it\,js}^{f}$) as:

$$\gamma_{it\,js}^{f} = \begin{cases} -M & \text{if } l_{it\,js} > 0, \\ c_{ij}^{d} & \text{otherwise}, \end{cases} \quad \forall (i,t,j,s) \in \mathbf{A};$$

Step 2.2. Set $L_{i_O t_O}^{f} = 0$;

Step 2.3. Do for each space-time arc $(i,t,j,s) \in \mathbf{A}$:

if $L_{it}^{f} + \gamma_{it\,js}^{f} < L_{js}^{f}$, then update the traveling cost state as $L_{js}^{f} = L_{it}^{f} + \gamma_{it\,js}^{f}$ and update the previous station and time of space-time vertex (j,s) as $PN_{js}^{f} = i$ and $PT_{js}^{f} = t$;

Step 2.4. Select $L_{i^*(t_0+M\delta)}^{f} = \min\{L_{i(t_0+M\delta)}^{f}\}_{i \in \mathbf{I}}$;

Step 2.5. Track back from space-time vertex $(i^*, t_0 + M\delta)$ to dummy origin vertex (i_O, t_O) using the values of PN_{it}^{f} and PT_{it}^{f}, and record all the relative space-time arcs in set $\mathbf{P}_f$;

Step 2.6. Do for each $(i,t,j,s) \in \mathbf{P}_f$:

If $l_{it\,js} > 0$, then update $l_{it\,js}$ as $l_{it\,js} = l_{it\,js} - 1$;

Step 2.7. Update $\bar{\mathbf{F}} = \bar{\mathbf{F}} \backslash \{f\}$ and repeat Step 2;

Step 3. Obtain the feasible solution $\bar{\mathbf{Z}}$ as:

$$\bar{Z}_{it\,js}^{f} = \begin{cases} 1 & \text{if } (i,t,j,s) \in \mathbf{P}_f, \\ 0 & \text{otherwise}, \end{cases} \quad \forall (i,t,j,s) \in \mathbf{A}, f \in \mathbf{F};$$

Step 7. Return the feasible solution $\bar{\mathbf{Z}}$.

draw some managerial insights into optimal strategies of EVSR. Eventually, a series of sensitive analyses are conducted in Section 5.3 to explore how the key parameters affect the optimal allocation and operation design of the one-way carsharing system.

5.1. Illustrative cases

Here, we first consider a set of illustrative numerical examples, through which we compare the Lagrangian relaxation-based solution approach (termed as LR in the following content) with two widely used commercial solvers, i.e., CPLEX (12.3 Academic Version) and Gurobi (7.0.1 Academic Version). The option parameters of these two solvers are set to default values. In addition, all the experiments are conducted on a personal computer with 3.4 GHz CPU and 8 GB RAM.

5.1.1. Parameter settings

In this numerical experiment, we consider a set of instances with different numbers of parking stations, time horizons, user trips, EVs and staff. To better illustrate the parameter settings of each instance, we use an instance index, i.e., P-T-U-V-F, in which these letters respectively denote the total numbers of parking stations, timestamps, user trips, EVs and staff members in the formulated space-time network. Each time interval in the space-time network is set as 10 minutes. Note that the user trips are randomly distributed in the space-time network. For example, Fig. 5 illustrates the parameter settings of instance 5-10-10-10-5, which involves 5 parking stations, 10 timestamps (i.e., 90 min), 10 reserved trips, 10 EVs and 5 staff members in this experiments. The link travel time and distance between two stations are also given on each dashed arrow line. Distance d_{ij} between two stations $i, j \in \mathbf{I}$ is generated randomly in interval [5,15], and the link travel time is populated as $T_{ij} = \lceil d_{ij}/5 \rceil$.

In addition, all the parking stations are assumed to be uniformly equipped with level 2 chargers that offer a battery charging rate $E^{+} = 1$ kW·h per unit time (i.e., 10 min). Since this study assumes that all the considered EVs are in the

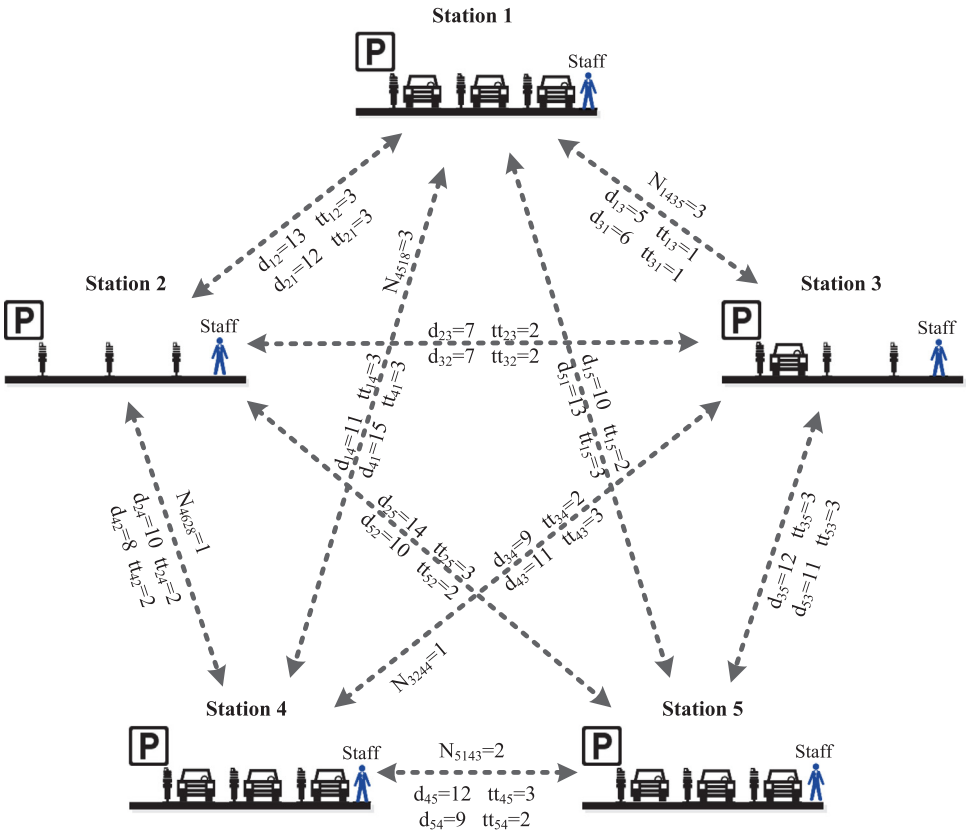

Fig. 5. An illustration of instance 5-10-10-10-5.

same working condition, we unify all the EVs as Smart For two electric drive (or Smart ED) with the battery capacity E_0=9 kW · h and the battery consuming rate E^- =0.5 kW · h per unit time.[3] The amortized cost (i.e., the EV investment cost that is divided in each day) for each EV c^a=\$130/day. The traveling cost of EVs is composed of the estimated electric charging cost (\$0.05/km) and estimated depreciation cost (\$0.1/km). Then we have c^l_{ij} =0.15d_{ij}. The daily salary of each staff member is set as c^y=\$150, and the staff relocation cost is set as \$0.5/km, i.e., c^d_{ij} =0.5d_{ij}.

5.1.2. Performance analysis of our proposed approach

To test the performance of our proposed approach, we test a total of 12 instances at different scales with CPLEX, Gurobi and LR. In particular, we repeat each instance for 10 times with random generated user demand and link travel time (see Section 5.1.1 for details). In these experiments, the parameter settings of LR algorithm are set as follows. Parameter τ^k is initially set to 2.0, and then decreases according to the lower bound updating tendency (see Algorithm 5). The algorithm terminal parameters are set as $\epsilon = 0.1$, $\overline{\tau} = 10^{-3}$ and $\overline{K} = 1000$, respectively.

We present the minimum, maximum and average solution times and optimality gaps for each instance by CPLEX, Gurobi and LR. Since the maximum computational time limit is set as 3000 seconds, we terminate these solution approaches and report the returned optimality gap. For the LR algorithm, the optimality gap is calculated by $(UB - LB)/UB \times 100\%$, where *UB* and *LB* respectively denote the best lower bound and upper bound encountered up to the current iteration (Cui et al., 2016). If these is no feasible solution in 3000 seconds, we report the gap as "NA".Note that for the cases in the same scale, the difference of user demand distribution actually will not much affect the performance of the solvers. Therefore, the "NA" means that no feasible solution can be obtained from any case in this instance. In addition, we also present the average lengths of user trips (termed as D_{user}) and average distances between any two stations (termed as $D_{station}$) for each instance.

We can see from Table 1 that all these solution approaches (i.e., LR, CPLEX and Gurobi) take longer solution times with the increase of instance scale. Nevertheless, the solution performances of CPLEX and Gurobi degenerate much faster than the LR algorithm. For the relatively small-scale instances, e.g., instances 5-10-10-10-5 and 10-10-10-10-5, all the solution approaches can yield a near optimal solution with an optimality gap of $< 0.1\%$ in a short solution time, and the LR algorithm even takes a little longer solution time than these two commercial solvers. When the instance scale increases, we see the

[3] https://en.wikipedia.org/wiki/Smart_electric_drive.

Algorithm 5 LR algorithm for EVSR problem in one-way carsharing systems.

Step 1. Initialize:
(a) $\{(\lambda_{itjs})^{k=0}\}_{(itjs)\in\mathbf{A}} = 0$ and $\{(\mu^h_{itjs})^{k=0}\}_{(itjs)\in\mathbf{A},h\in\mathbf{H}} = 0$;
(b) $\tau^{k=0} \in (0, 2]$;
(c) $UB^{k=0} = +\infty$;
Step 2. Calculate the optimal solution $LB^k(\boldsymbol{\lambda}, \boldsymbol{\mu})$ of the relaxed model by using Algorithms 1–2, and then obtain the relaxed solutions $\hat{\mathbf{X}}^k$, $\hat{\mathbf{Y}}^k$ and $\hat{\mathbf{Z}}^k$
Step 3. Calculate the feasible solutions by using Algorithms 3–4, and then update LB^k to the relative feasible objective if LB^k is greater than it;
Step 4. Calculate the step size t_k by Equation (30);
Step 5. Update the Lagrangian multipliers by Equations (28) and (29);
Step 6. Go to Step 7 if satisfying one of the following conditions; otherwise, set $k \leftarrow k + 1$ and go to Step 2;
(a) optimality gap $\frac{UB^k - LB^k(\boldsymbol{\lambda},\boldsymbol{\mu})}{UB^k} \leqslant \epsilon$, where ϵ is a pre-specified error tolerance;
(b) τ^k is smaller than a minimum value $\overline{\tau}$;
(c) k exceeds a maximum iteration number $\overline{K}$;
Step 7. Terminate this algorithm and return the current best feasible solution as the near-optimum solution.

Table 1
Performance comparison of different solution approaches.

Instance	D_{user}(km)	$D_{station}$(km)	Value	Solution time (sec)			Gap (%)		
				LR	CPLEX	Gurobi	LR	CPLEX	Gurobi
5-10-10-10-5	10.05	9.95	Min	9.47	5.02	4.58	< 0.1	< 0.1	< 0.1
			Ave	10.16	6.44	5.79	< 0.1	< 0.1	< 0.1
			Max	12.05	7.27	6.13	< 0.1	< 0.1	< 0.1
5-30-30-30-15	10.03	9.95	Min	125.30	> 3000	2987.92	2.44	8.03	8.03
			Ave	127.91	> 3000	> 3000	3.73	8.59	8.11
			Max	131.17	> 3000	> 3000	4.08	9.24	8.80
5-60-60-60-30	9.65	9.95	Min	677.35	> 3000	> 3000	2.83	NA	NA
			Ave	690.07	> 3000	> 3000	4.01	NA	NA
			Max	721.02	> 3000	> 3000	4.96	NA	NA
10-10-10-10-5	11.80	9.92	Min	20.90	18.32	20.18	< 0.1	< 0.1	< 0.1
			Ave	21.87	19.03	20.89	< 0.1	< 0.1	< 0.1
			Max	23.06	20.94	21.75	< 0.1	< 0.1	< 0.1
10-30-30-30-15	10.30	9.92	Min	375.98	> 3000	> 3000	3.91	10.72	10.32
			Ave	395.52	> 3000	> 3000	4.44	11.03	10.80
			Max	420.66	> 3000	> 3000	5.28	11.81	11.22
10-60-60-60-30	10.52	9.92	Min	963.67	> 3000	> 3000	4.63	NA	NA
			Ave	989.27	> 3000	> 3000	5.32	NA	NA
			Max	1004.53	> 3000	> 3000	7.38	NA	NA
20-10-10-10-5	9.40	10.05	Min	63.07	224.67	397.01	< 0.1	< 0.1	< 0.1
			Ave	68.39	228.52	401.24	< 0.1	< 0.1	< 0.1
			Max	77.29	230.86	405.70	< 0.1	< 0.1	< 0.1
20-30-30-30-15	10.08	10.05	Min	1040.01	> 3000	> 3000	4.55	NA	NA
			Ave	1058.84	> 3000	> 3000	5.12	NA	NA
			Max	1073.11	> 3000	> 3000	6.09	NA	NA
20-60-60-60-30	10.09	10.05	Min	2341.85	> 3000	> 3000	6.62	NA	NA
			Ave	2369.57	> 3000	> 3000	7.91	NA	NA
			Max	2384.43	> 3000	> 3000	9.88	NA	NA
30-10-10-10-5	10.20	9.95	Min	145.03	628.92	462.21	< 0.1	< 0.1	< 0.1
			Ave	151.88	630.77	466.09	< 0.1	< 0.1	< 0.1
			Max	155.54	635.10	469.73	< 0.1	< 0.1	< 0.1
30-30-30-30-15	10.16	9.95	Min	1127.24	> 3000	> 3000	7.24	NA	NA
			Ave	1149.68	> 3000	> 3000	9.89	NA	NA
			Max	1173.03	> 3000	> 3000	11.79	NA	NA
30-60-60-60-30	9.96	9.95	Min	> 3000	> 3000	> 3000	8.08	NA	NA
			Ave	> 3000	> 3000	> 3000	10.32	NA	NA
			Max	> 3000	> 3000	> 3000	12.04	NA	NA

noticeable advantage of the LR algorithm because it can still solve the instances to high-quality solutions (with optimality gap no more than 8%) within a reasonable solution time, whereas the performance of CPLEX and Gurobi become extremely unreliable. For the medium scale instances, such as instances 5-30-30-30-15 and 10-30-30-30-15, these two solvers both yield over 8% gap in a solution time of more than 3000s. For the large scale instances, e.g., instances 30-30-30-30-15 and 30-60-60-60-30, the solvers cannot even obtain a feasible solution. Therefore, it is reasonable to draw the conclusion that the performance of our proposed LR algorithm is significantly better than the commercial solvers in solving EVSR models.

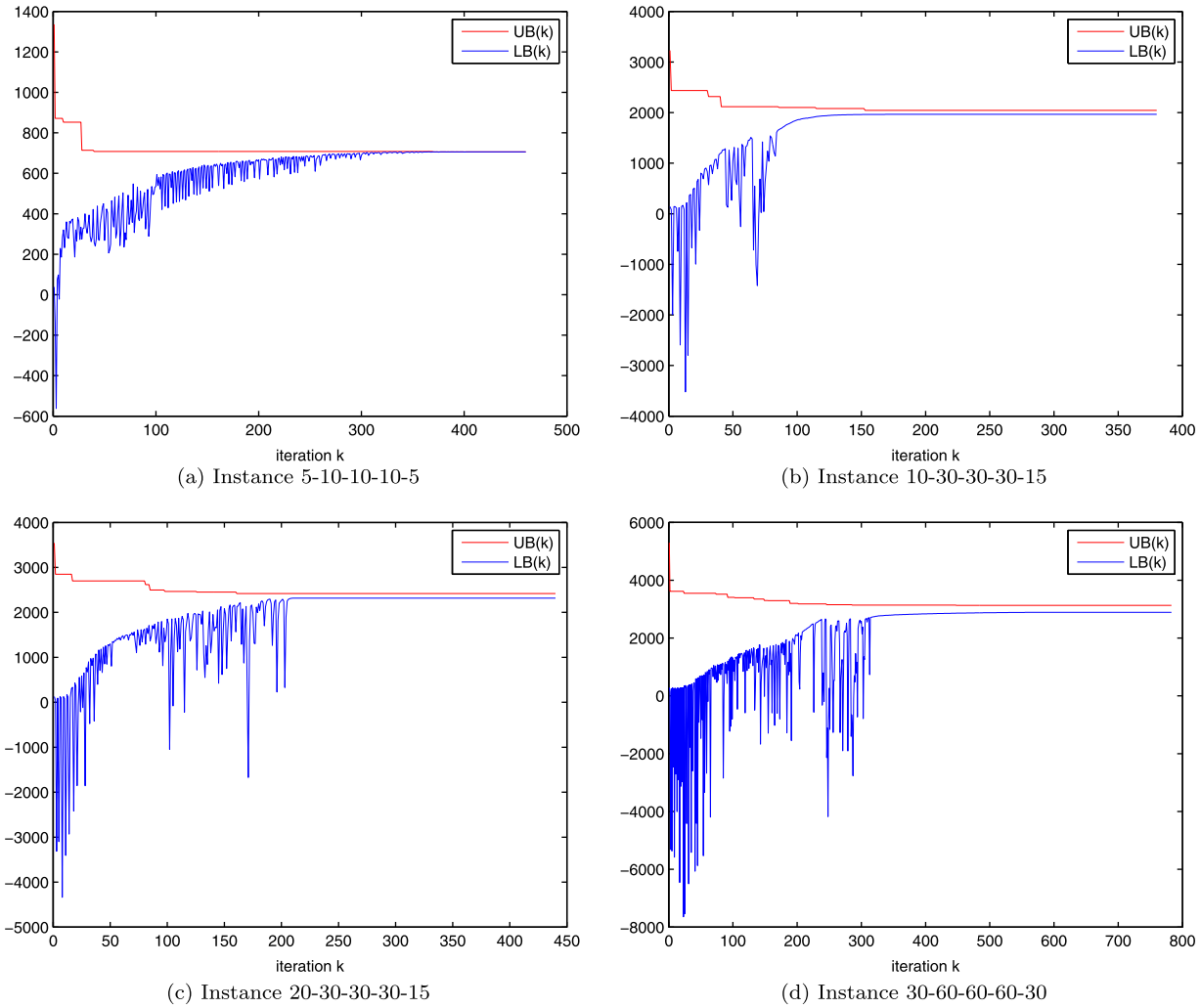

(a) Instance 5-10-10-10-5

(b) Instance 10-30-30-30-15

(c) Instance 20-30-30-30-15

(d) Instance 30-60-60-60-30

Fig. 6. Tendencies of UB and LB for different scales.

Moreover, we see that the minimum, maximum and average values of solution times and gaps are relatively stable by these three solution approaches in each instance, which can demonstrate that our approach is not sensitive with the random distribution of user reservation and link trip time.

In addition, Fig. 6 shows the convergence tendency of the best upper bound and lower bound for one experiment in instances 5-10-10-10-5, 10-30-30-30-15, 5-10-10-10-5 and 30-60-60-60-30. We can see clearly that these two bounds get closer rapidly at first, then the convergence tendency slows down, and finally the algorithm is terminated with best feasible solution returned if any of the termination conditions are reached. We need to note that, the upper and lower bound iteration trends also indicate that the quality of the solution may not be much effected as we properly reduce the number of iterations. This property will help to save the solution time for the cases that require a faster solution speed without as high solution quality.

5.1.3. Objective values of EVSR with different numbers of user reservations

Here, we particularly address a specific case with 5 parking stations, 30 time intervals, 40 EVs and 20 staff members (see Fig. 5) to test how the operation costs vary with different numbers of user reservations. In order to evaluate the objective components of each instance, we use C, C^H, C^Y, C^L and C^D to denote the total cost, EV amortized cost, staff hiring cost, EV traveling cost and staff relocation cost, respectively. The number of user trips in the first instance is set as 20, and we add 20 more trips to each instance afterwards. The other model parameters and the LR algorithm parameters are all set the same as Section 5.1.1 and Section 5.1.2. We also repeat each instance for 10 times with different random generated user demand samples and we present the average values of these indicators in Table 2.

Table 2 presents the objectives of 10 instances from 20 reservations to 200 reservations, where the objectives in each instance are taken as average values by 10 times of repeated experiments. It is obvious that all the objective values grad-

Table 2
Objective values for investment and operation costs of EVs and staff.

Instance index	C^H	C^Y	C^L	C^D	C	Gap (%)
5-30-20-40-20	1183.0	270.0	35.6	12.1	1500.7	0.85
5-30-40-40-20	1716.0	540.0	76.1	39.5	2371.6	5.98
5-30-60-40-20	2197.0	645.0	118.9	56.0	3016.9	8.83
5-30-80-40-20	2665.0	780.0	160.1	77.4	3682.5	10.20
5-30-100-40-20	3042.0	930.0	203.8	92.3	4268.1	12.67
5-30-120-40-20	3320.0	1080.0	245.8	107.1	4752.9	13.75
5-30-140-40-20	3354.0	1140.0	278.4	130.8	4903.2	17.05
5-30-160-40-20	3562.0	1230.0	311.6	144.9	5248.5	22.08
5-30-180-40-20	3653.0	1350.0	343.5	129.7	5476.2	27.07
5-30-200-40-20	3744.0	1350.0	369.7	130.5	5594.2	31.55

ually increase with more user reservations, which is actually consistent with our practical experience that more EVs and staff members are required to meet the increased user activities. An interesting phenomenon is that the total cost is only increased from 1500 to 5594 as the number of user reservations is added from 20 to 200. The nonlinear relationships between user demands and cost components can indicate that the properly designed EVSR strategies can dramatically save the investment and operation costs of carsharing companies through the relocation of EVs and rebalancing of staff members. With respect to the computational efficiency, we find that the LR algorithm can generate a good-quality solution and the returned gap is less than 25% when the amount of user reservations is lower than 180. For more reservations (i.e., instances 5-30-180-40-20 and 5-30-200-40-20), the performance of LR algorithm gradually becomes a little worse and the obtained solution has about 30% gap, which is essentially due to the relaxation of user flag variables in the LR algorithm that make it difficult to assign more users to their corresponding EVs. Moreover, we also find that when the number of user reservations is increased to 230, there is no feasible solution that can be obtained, which means that 230 user reservations are oversaturated conditions to the carsharing system with 5 stations, 30 timestamps, 40 EVs and 20 staff members, which is actually out of scope of this paper.

Besides, to show more detailed properties of EVSR by the LR algorithm, we further define four more performance indicators, i.e., the EV utility rate (denoted by μ), staff utility rate (denoted by ρ), number of used EVs and number of rebalancing tasks of each staff member. Similarly to the definition by Boyacı et al. (2017), the EV and staff utilities are here represented as the ratios of average traveling time of each EV and staff member with respect to the duration of an operation cycle, explicitly given as

$$\mu = \frac{\text{Total traveling time of EVs}}{|\mathbf{T}| \times \sum_{i \in \mathbf{I}} H_i} \quad \text{and} \quad \rho = \frac{\text{Total traveling time of staff members}}{|\mathbf{T}| \times \sum_{i \in \mathbf{I}} F_i}.$$

It is clear that larger μ and ρ could correspondingly indicate the better utilization of EV and staff investments, and potentially raise the profits of carsharing company. Note that $\Sigma_{i \in \mathbf{I}} H_i$ and $\Sigma_{i \in \mathbf{I}} F_i$ in these two equations represent the numbers of EVs and staff members that are engaged during the operation cycle, which are less than (or equal to) the maximum numbers.

The variations of these indicators with respect to the growth of user demands (corresponding to the instances in Table 2) are shown in Fig. 7. We can see from the results that the variations of these four indicators present the similar trends, and they generally increase with more user reservations. In particular, the utility of EVs and staffs can be as high as 80% when there are more than 180 user reservations, which possibly reveals the fact that, with large scales of EVs and staff in a one-way carsharing system, the flexibility of EV rebalancing and staff relocation operations would be greatly improved, and the growth number of user reservations can be better covered with the well planned EVSR strategies. In addition, it can be observed from Fig. 7(b) and Fig. 7(d) that, the fluctuation of staff utility and number of rebalancing tasks per staff member for each instance is much more evident with respect to the random distributed user reservations. This demonstrates that the operational strategies of staff members are more sensitive to the distribution of user activities and should be paid more attention in making EVSR plans. Besides, to show more details about the solutions, we specially select a case in instance 5-30-200-40-20 as an illustrative example to present the user reservations, the space-time trajectories of EVs and staff members in the space-time network, which is shown as Fig. C.12 in Appendix C.

5.2. Real-world case study

Conducted by some carsharing companies (e.g., ZipCar), one-way carsharing systems have been put into trial operations in many large cities (such as Seattle, Boston and Denver in the United States; Beijing, Shanghai in China; Toronto in Canada). In the following case studies, we particularly use the one-way carsharing system of Seattle, WA, to test our proposed EVSR model and solution approach.

As shown in Fig. 8, we first aggregate the parking spots into 26 equivalent parking stations in Seattle area, which are marked as green icon. The travel distance d_{ij} and travel time T_{ij} are generated by the distance and daily average travel time through the shortest path between two parking stations i and j, and the average distance between any two stations is

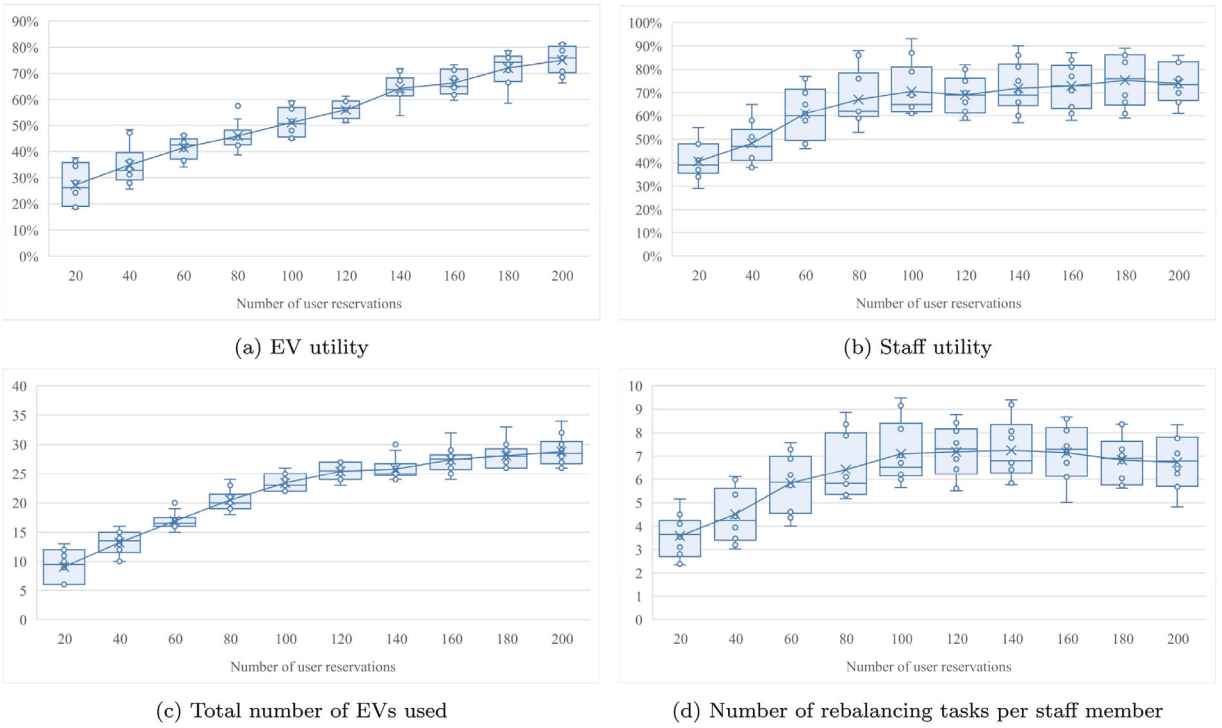

Fig. 7. Variations of some performance indicators with respect to the growth of user demand.

Table 3
Performance comparison of LR and LR-BB in solving real-word cases.

Instance	N_{total}	D_{user}(km)	Max #	Station index	Solution time (sec)		Gap (%)	
					LR	LR-BB	LR	LR-BB
1	122	7.96	5	17,26	3392.28	3457.16	16.60	14.82
2	134	7.77	5	15	3517.99	3382.04	27.31	22.47
3	141	8.55	6	17,21	3845.03	3802.53	30.28	25.06
4	126	8.63	4	21,9	3596.20	3627.84	20.89	16.00
5	148	8.04	6	17,15	4013.56	4101.79	33.71	29.93

8.06km. In each weekday, we set the operation cycle to be 12 hours (i.e., 7:00 am-7:00pm) and each time interval covers 10 minutes. That is, the constructed space-time network consists of 72 time intervals in total. Additionally, we set the maximum numbers of EVs and staff as $H_{\max}$ =130 and $F_{\max}$ =60, respectively. To track the practical tide phenomenon in morning and evening peak hours, we randomly generate 5 groups of dynamic user reservations for the following experiments. Each group of data has high demands in peak hours and relatively low demands in off-peak hours, as shown in Fig. 9. Furthermore, to analysis the impact of gravitational effect on the whole system, we assume stations 15,17, 21 and 26 as the "core stations" that act as the origin or destination stations of most user tips during the peak hours. The other parameter settings are the same as those in Section 5.1. Besides, to further improve the performance of our LR-based solution approach in solving these large-scale real-word cases, we also integrate the LR algorithm into a branch and bound framework (LR-BB), which is similar to the treatment by Cui et al. (2016) and Yang and Zhou (2014). The general procedure of LR-BB can be seen in Appendix D.

Table 3 presents the total number of user reservations, average travel distance of users and the performances of LR and LR-BB for these five instances. Besides, to demonstrate the sensitivity of the results to the capacity limit, we also present the maximum number of EVs that dwell at a station in the same time unit (termed as Max #), as well the indexes of the corresponding stations (termed as Station index) for LR and LR-BB. We can see that the Max # is no more than 6 in these instances, which is actually not beyond the capacity of the parking station in most carsharing systems (e.g., the TOGO station in Beijing). The solution time of both LR and LR-BB is about 1 h, and the optimality gap varies from 10% to 34%. In particular, the returned gap is much larger when the number of user reservations is higher, which is consistent with the previous observation that the Lagrangian relaxation approach is relatively sensitive with the amount of user reservations. In addition, it is obvious that LR-BB is a little better than LR with respect to the returned optimality gap while consuming nearly the same computational time, which illustrates the effectiveness of LR-BB. Hence, we implement the LR-BB algorithm for the following real-world experiments.

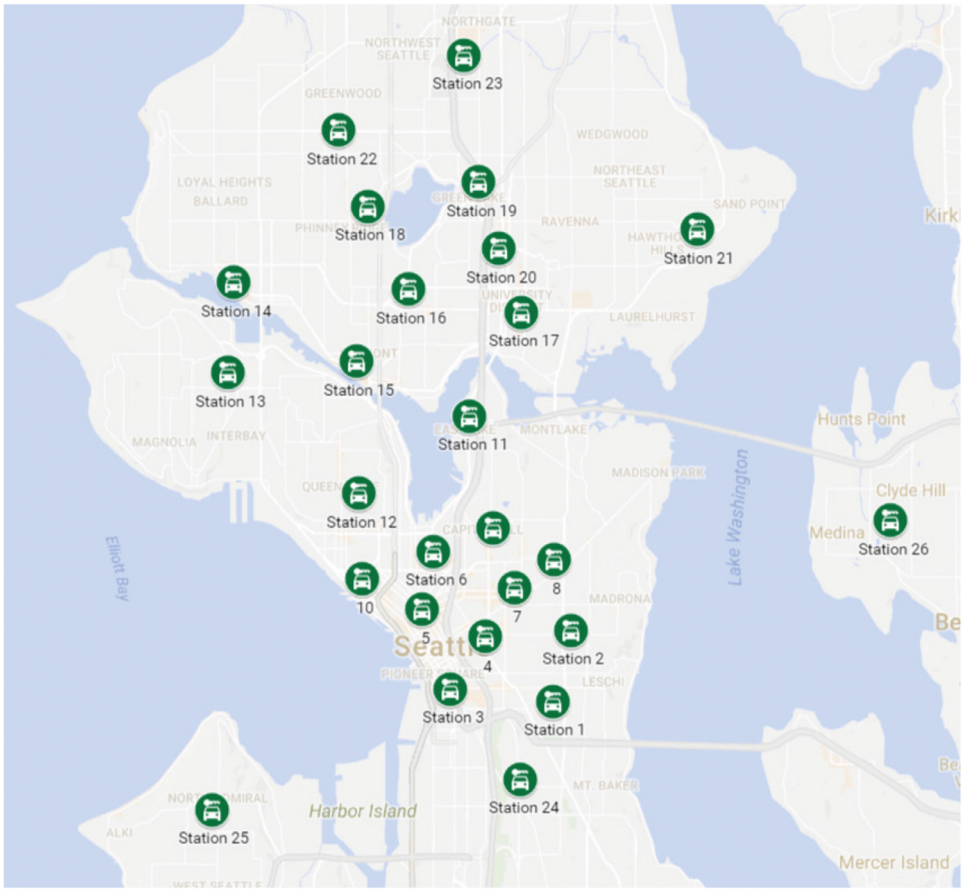

Fig. 8. Locations of parking station anchors in Seattle.

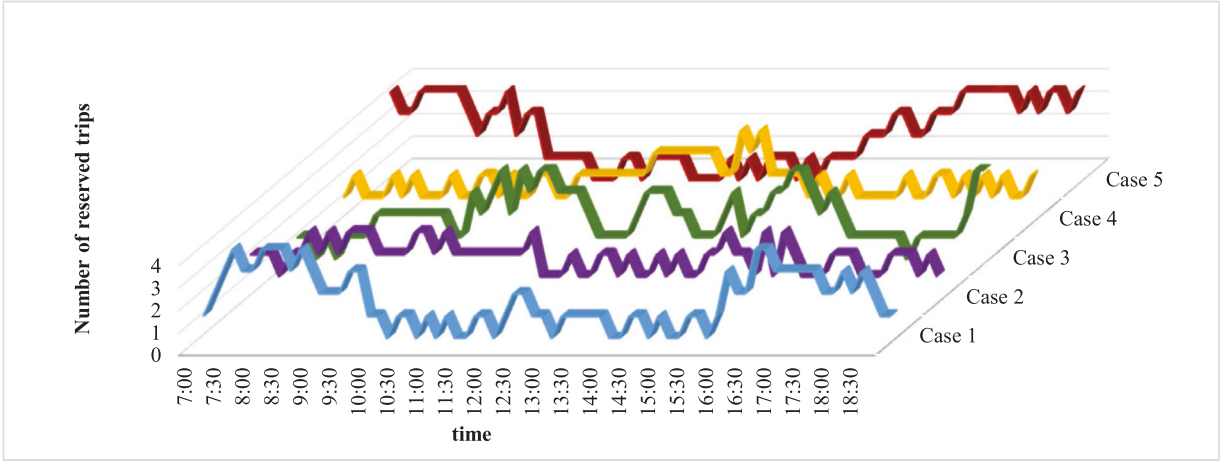

Fig. 9. User demands variation through the time horizon.

Furthermore, we particularly present the EVSR allocation plans (see Fig. 10a) and dispatching strategies (see Fig. 10b–10 d) for instance 1 in Table 3 using our proposed LR-BB algorithm. More specifically, Fig. 10a demonstrates the numbers of allocated EVs and staff members to each station at the initial time, which are respectively represented by blue and orange cylinders, and the height of each cylinder is proportional to the number of EVs or staff members. Fig. 10b–10 d illustrate the EV rebalancing and staff relocation strategies for morning peak hours (7:00am - 9:30am), off-peak hours (9:30am - 4:00pm) and evening peak hours (4:00 pm–7:00 pm), respectively. In these figures, the numbers marked on the arrows represent the

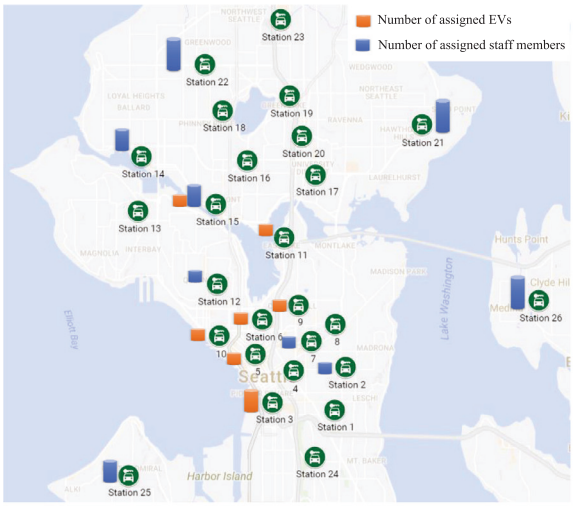

(a) Allocation plan of EVs and staff to parking stations

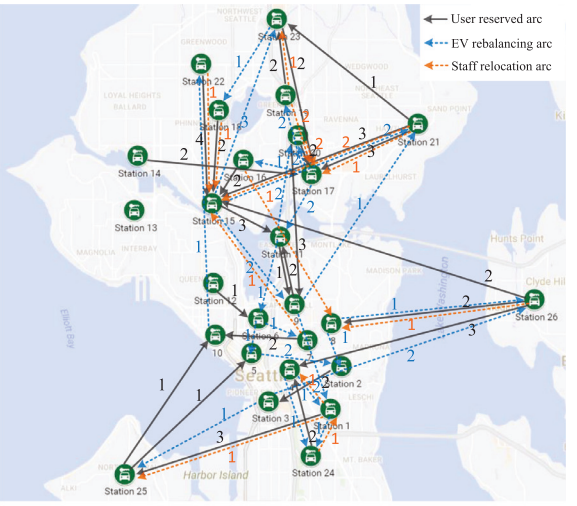

(b) EV relocation and staff rebalancing operations in 7:00am - 9:30am

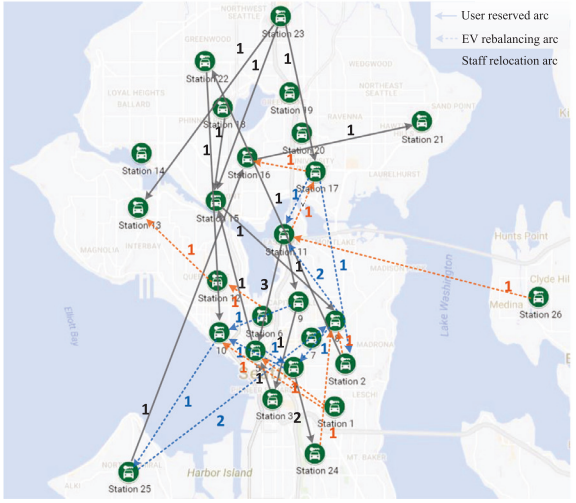

(c) EV relocation and staff rebalancing operations in 9:30 - 4:00pm

(d) EV relocation and staff rebalancing operations in 4:00pm - 7:00pm

Fig. 10. Optimal allocation plans and operation strategies of EVs and staff in the case study of Seattle.

corresponding numbers of trips. The black solid, blue dash and orange dash arrows refer to the user reserved trips, the EV rebalancing trips and the staff relocation trips, respectively.

We see from Fig. 10a that, most of the staff are initially allocated to parking stations in downtown areas while most of the EVs are allocated to the suburban parking stations. This distinct characteristic of EV and staff allocation layout is possibility caused by the typical tide phenomenon that more users travel from suburban areas to downtown areas during morning peak hours. Fig. 10b illustrates the following two phenomena. (1) Since more EVs are driven to downtown districts by users, there is an opposite tendency that most rebalanced EVs are from the downtown parking stations (e.g., stations 15 and 17) towards suburban parking stations (e.g., stations 20, 21 and 26). This is essentially caused by the continuous higher demands of EVs in suburban areas during this time period. (2) Meanwhile, the staff relocation tasks are carried out in a similar way to the traveling directions of users. This is actually due to that, after finishing the EV rebalancing operations to the suburban areas, these staff then return back to the downtown area for the next “rebalancing-relocation cycle”.

In Fig. 10c, we see that there are much less user trips occurring in this time period (i.e., time 9:30 am to 4:00 pm), and accordingly, fewer EV rebalancing operations are observed in comparison with Fig. 10b. The reason is that, the OD demand during off-peak hours is relatively low and evenly distributed among stations, and in this sense, the balance of EV numbers among these stations could be easily kept with less frequent relocations. In addition, we can see an interesting phenomenon that the staff gradually move toward the north part of this city (e.g., station 13, 15, 16, 17) during this time period, which possibly indicates that they are preparing for rebalancing EVs in the evening peak hours.

From Fig. 10d, we see the generally opposite tendency of the trips of users, EV rebalancing and staff relocation with respect to that in Fig. 10b. In specific, most users travel from downtown to suburban districts in evening peak hours, which

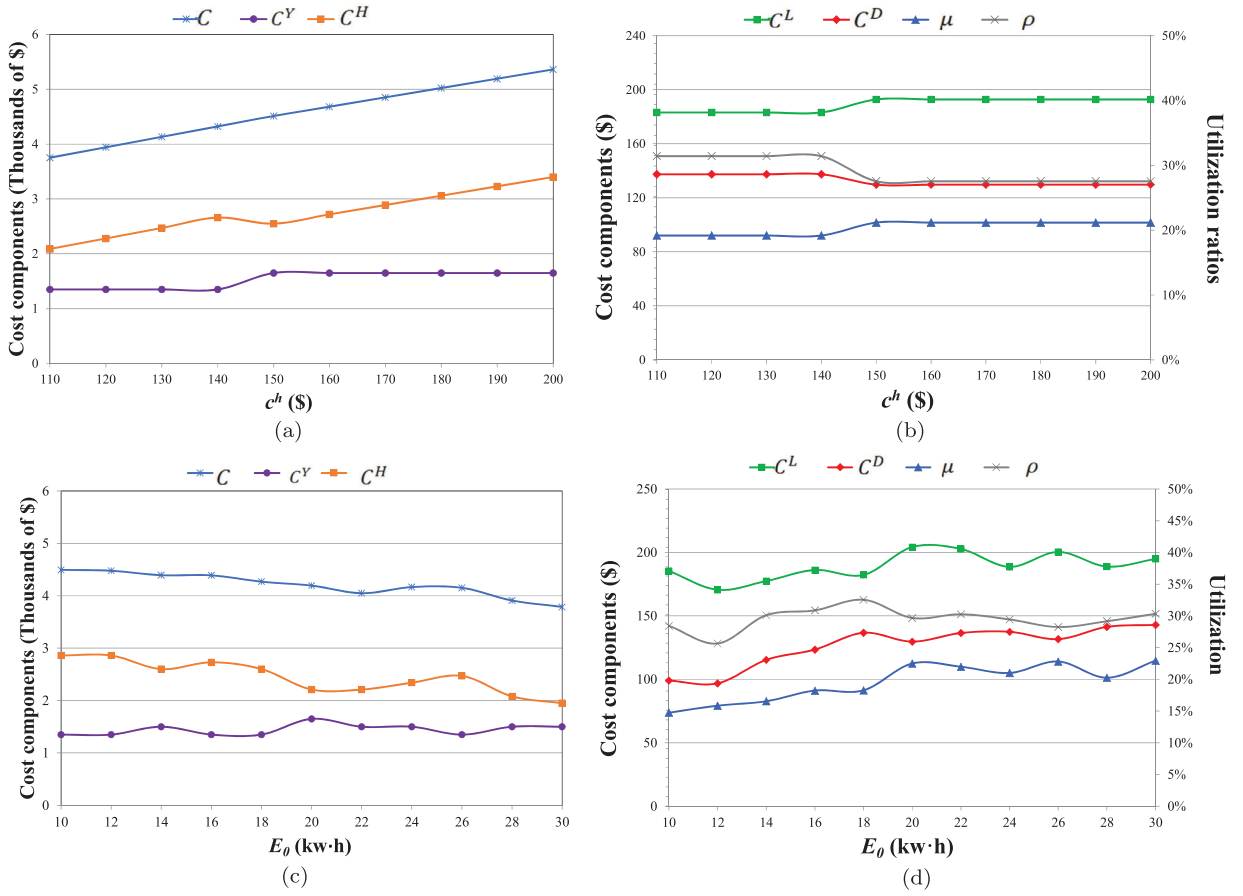

Fig. 11. Sensitivity analyses on model parameters c^a and E_0.

is also caused by the tide phenomenon in contrast with morning peak hours. Due to this reason, we can see that most of the EV rebalancing and staff relocating tasks are also operated oppositely with those in morning peak hours.

Based on the experimental results above, we can summarize the following managerial insights: (1) For the allocation plans of EVs and staff, more EVs are needed in the suburban parking stations at the initial time, while most of staff should be allocated to downtown parking stations. This would be an effective and economic strategy to handle the user reservations with destinations to downtown areas during morning peak hours. (2) For the EVSR strategies during the operation cycle, the numbers of EV rebalancing and staff relocation tasks are generally proportional to the total number of corresponding user trips. For instance, fewer EV rebalancing and staff relocation tasks are observed during off-peak hours comparing with those in peak hours. The implication of this result is that the carsharing manager can potentially make better operation strategies to save staff hiring cost, e.g., hiring less working staff in off-peak hours according to the specific user reservations.

5.3. Model sensitive analysis with different parameter settings

In this section, we perform a series of numerical experiments to verify how the key parameters affect the optimal EVSR objectives based on the real-world case (instance 1) in Section 5.2. Indicators C, C^H, C^Y, C^L, C^D, μ and ρ in this set of experiments, which are defined the same as those mentioned in Section 5.1.3, represent the total cost, EV amortized cost, staff hiring cost, EV traveling cost, staff relocation cost, EV utility rate and staff utility rate, respectively. (See Appendix E for the definition of indicators) In addition, we set all the benchmark parameter values the same as those in Section 5.2 and only one specified parameter value varies in each experiment.

In practice, an important issue in EV carsharing systems is the high investment cost of EVs. Thus, we first conduct a set of experiments with different EV investment costs in order to investigate the influence of EV investment cost on the optimal EVSR strategies. Fig. 11a and Fig. 11b demonstrate the variations of all the performance indicators with increased amortized cost of each EV from \$110 to \$200. We see from them that when c^a grows from 110 to 140, C^H increases rapidly, which dominates the increasing trend of C. Meanwhile, all the other indicators are relatively stationary. As c^a continues to rise, the total cost C keeps growing consistently. Nevertheless, C^H has a sharp drop when c^a reaches 150, and then it keeps growing as well. At the same time, C^Y increases from around 1200 to 1700 and then flattens out. The reason is that, as the EV

investment cost grows, reducing the fleet size and hiring more working staff become a more economical strategy to offset the growth of total EV amortized cost. Accordingly, C^L, μ, C^D and ρ demonstrate the similar tendency in Fig. 11b: C^L and μ increase a little while C^D and ρ drop a little when c^a reaches 150. This is because that, with less EVs and more staff, the existing EVs are rebalanced more frequently in order to meet the user reservations, which actually raises the EV traveling cost and utilization ratio of EVs. Meanwhile, the utilization ratio of staff and the staff relocation cost are reduced accordingly. The results essentially imply the intrinsic trade-off relationship between these two indicators, i.e., the investment costs on purchasing EVs and hiring staff.

On the other hand, a key indicator that evaluates the performance of EVs is the battery capacity, which also has a significant impact on the optimal EVSR strategies. To this end, we test the variations of the performance indicators with the magnitudes of battery capacity E_0. The results are shown in Fig. 11c and Fig. 11d. In Fig. 11c we see that when E_0 raises from 10 to 30, C^Y generally remains the same value with small fluctuations, while the decrease of C^H dominates the dropping trend of C. This indicates that, higher battery capacity increases the total travel distance of EVs, which also reduces the fleet size of EVs, and thus decreases the investment cost C^H. We also see in Fig. 11d that all these indicators have evident increases with the growth of E_0. This is clearly because that: (1) In order to satisfy the user reservations with a decreased number of EVs, more EV rebalancing tasks are needed, leading to the increase of the rebalancing cost C^L and utilization ratio of EVs μ. Accordingly, more staff members are also required, which dramatically brings down the staff relocation cost C^D and utilization ratio of staff ρ. (2) Higher battery capacity would also increase the service time of each EV without frequent recharges, which also enables each staff member to do more rebalancing operations flexibly to offset the decreased number of EVs. This could also well explain the reason why staff hiring cost C^Y (i.e., staff size) remains nearly the same in spite of the decreased number of EVs.

6. Conclusion

In this paper, we studied the integrated EV rebalancing and staff relocation problem in one-way carsharing systems. By using a space-time network representation, the EVSR problem was formulated into a mixed integer linear programming (MILP) model that synchronously considers the dynamic user reservations, limited EV battery capacity and EV charging time at parking stations. The aim is to determine the optimal EV and staff lay out with the consideration of EV rebalancing and staff relocation plans that satisfy user demands with the least total cost of carsharing companies. Since the model is essentially formulated as a multi-vehicle routing problem and contains complex coupling constrains, it is actually very difficult to handle with existing commercial solvers. Hence we particularly developed a customized solution approach based on Lagrangian relaxation embedded with forward DP and branch-and-bound in order to solve this model more efficiently and accurately.

A series of numerical studies were conducted based on two cases, i.e., an illustrative case and a real-world case of Seattle carsharing system. The computational results showed that, for medium-scale instances, the developed LR algorithm can obtain near-optimum solutions with a small optimality gap in a much shorter computational time than CPLEX and Gurobi solvers. In particular, for large-scale instances, neither of the two solvers can provide even a feasible solution, while the developed LR algorithm can still obtain a good solution in an acceptable time. Besides, based on the real-world case study, we specifically analyzed the optimal EV rebalancing and staff relocation strategies in different time periods during a typical work day. We also drew some managerial insights on the effects of key parameters to the system performance indicators. For example, we derive the relationship between EV battery capacity and the service frequency of EVs, which indicates that higher EV battery capacity can save more EVs investment cost with nearly the same staff size.

This study proposed an open-ended carsharing system operation design framework that can be extended in several directions for the future research. (1) In this study, we assume that each carsharing station can hold and charge as many EVs as possible. Nevertheless, the facility construction cost, which limits the numbers of parking ports and charging piles in real-world cases, is actually an important component that shall also be considered in the long-term planning stage. Hence, an interesting extension of this study is the simultaneous optimization approach that incorporates the parking station design for carsharing systems. (2) This study assumes that the link travel time between two stations is constant with time and the battery charging and consuming processes are discrete with respect to only time durations. These assumptions suffice certain cases where the travel time on each time is relatively predictable. When the actual travel times have random variations, the deterministic travel time in this framework can be also interpreted as the summation of the mean travel time and a safety gap that is sufficient to cushion travel time variabilities most of the time. Nonetheless, it will be interesting to investigate a microscopic approach to integrate the dynamics of link travel time and more detailed battery charging and consuming processes to this model framework. (3) Although we consider the user reservations as the typical-day-demand, the real-world characteristics of user demand is even more complex. In certain cases, some users may cancel the reservations just before the departure of their trips or put off the vehicle return time due to some unexpected reasons. Thus, another research direction is to extend our work to the area of robust design of carsharing system. Specially, the EVSR model could be adjust to a two-stage stochastic programming framework under scenario-based user demand and uncertain environment for providing a robust EVSR plan. (4) Besides, since battery volume variable is explicitly defined on every timestamp for each individual vehicle in the mathematical model, which essentially increases the computational intensity for solving large scale problems, another extension in the future research is to seek for better exact solution algorithms for solving huge problems more efficiently.

Table 4
Numerical results of solving EVSR-SC model in real-word cases.

Instance index	N_{total}	C	Solution time (sec)	Gap (%)
1	122	4132.6	> 3000	15.17
2	134	3881.2	> 3000	23.80
3	141	4479.0	> 4000	30.21
4	126	3620.2	> 3000	16.83
5	148	4776.6	> 4000	34.69

Acknowledgement

This research is supported in part by the Fundamental Research Funds for the Central Universities through Grant 2018RC024, by the National Natural Science Foundation of China through Grants 51478151, 61790570, 61790573, 71621001, 71531002 and 71421001, and by the US National Science Foundation through Grants 1638355, 1558889 and 1541130.

Appendix A. Illustrative cases for EVSR model with the station capacity constraints

To further evaluate the performance of the EVSR model adding the station capacity constraints (termed as the EVSR-SC model), a numerical experiment is executed based on the dataset of the real-word cases. In addition, the capacity of each station is set as 5. We here solve the EVSR-SC model by following the similar steps of LR-BB. The results are shown in Table 4.

We can see from Table 4 that the performance of LR-BB when solving EVSR-SC model is nearly the same as that of EVSR model for instance 1,2 and 4. However, the performance is much worse for instance 3 and 5. It is probably because that, when solving EVSR model, the max # are 6 in cases 3 and 5 (shown in Table 3), which exceeds the station capacity limits (i.e., 5 for each station). Therefore, when solving EVSR-SC model, much more constraints may be violated in the relaxed formulation during the iteration of LR-BB and it is more difficult to reduce the gap between the lower and upper bounds.

Appendix B. Proof of proposition 1

First, we set

$$C(\{Y^h_{it\,js}\}) = \sum_{(i,t,j,s)\in\mathbf{A}}\sum_{h\in\mathbf{H}}\mu^h_{it\,js}Y^h_{it\,js} + \sum_{(i,t,j,s)\in\mathbf{A}}(c^d_{ij}-\lambda_{it\,js})N_{it\,js}$$

and

$$\left\{\tilde{Y}^h_{itjs}\right\} := \text{argmin}C\left(\left\{Y^h_{itjs}\right\}\right).$$

Then we will prove $\{\tilde{Y}^h_{it\,js}\} = \{\hat{Y}^h_{it\,js}\}$ by contradiction. For any $(i,t,j,s)\in\mathbf{A}_u$, if there exists $\tilde{Y}^{h'}_{it\,js} = 1, h'\in\mathbf{H}\backslash\mathbf{H}^*_{it\,js}$ such that $\mu^{h'}_{it\,js} > \mu^{\hat{h}}_{it\,js}, \forall\hat{h}\in\mathbf{H}^*_{it\,js}$. We construct a new feasible solution $\{\acute{Y}^h_{it\,js}\}$ as:

$$\acute{Y}^h_{itjs} = \begin{cases} 1 & \text{if } h\in\mathbf{H}^*_{itjs}, \\ 0 & \text{otherwise}, \end{cases} \quad \forall h\in\mathbf{H},\ (i,t,j,s)\in\mathbf{A},$$

and then we compare the difference between the two objective function values with respect to $\{\tilde{Y}^h_{it\,js}\}$ and $\{\acute{Y}^h_{it\,js}\}$, respectively,

$$\begin{aligned} &C(\{\tilde{Y}^h_{it\,js}\}) - C(\{\acute{Y}^h_{it\,js}\}) \\ &= \sum_{(i,t,j,s)\in\mathbf{A}}\sum_{h\in\mathbf{H}}\mu^h_{it\,js}\tilde{Y}^h_{it\,js} + \sum_{(i,t,j,s)\in\mathbf{A}}(c^d_{ij}-\lambda_{it\,js})N_{it\,js} - \sum_{(i,t,j,s)\in\mathbf{A}}\sum_{h\in\mathbf{H}}\mu^h_{it\,js}\acute{Y}^h_{it\,js} - \sum_{(i,t,j,s)\in\mathbf{A}}(c^d_{ij}-\lambda_{it\,js})N_{it\,js} \\ &= \mu^{h'}_{it\,js} - \mu^{\hat{h}}_{it\,js}. \end{aligned}$$

Note that $\mu^{h'}_{it\,js} - \mu^{\hat{h}}_{it\,js} > 0$ due to the statement of the value of $\{\tilde{Y}^h_{it\,js}\}$ and $\{\acute{Y}^h_{it\,js}\}$. Then we obtain $C(\{\tilde{Y}^h_{it\,js}\}) > C(\{\acute{Y}^h_{it\,js}\})$, which is contradictive to the premise that $\{\tilde{Y}^h_{it\,js}\}$ is the optimal solution. This proves that$\{\tilde{Y}^h_{it\,js}\} = \{\hat{Y}^h_{it\,js}\}$, i.e., $\{\hat{Y}^h_{it\,js}\} :=$ argmin $C(\{Y^h_{it\,js}\})$.

Appendix C. Computational results of a case in instance 5-30-200-40-20

We specially select a case in instance 5-30-200-40-20 to show more details about the computational results, such as the user reservations, the space-time trajectories of EVs and staff members, which are shown in Fig. C.12. We can see from Fig. C.12 that 28 EVs and 9 staff members are finally put into use to fulfill 200 user reservations. Besides, we also execute

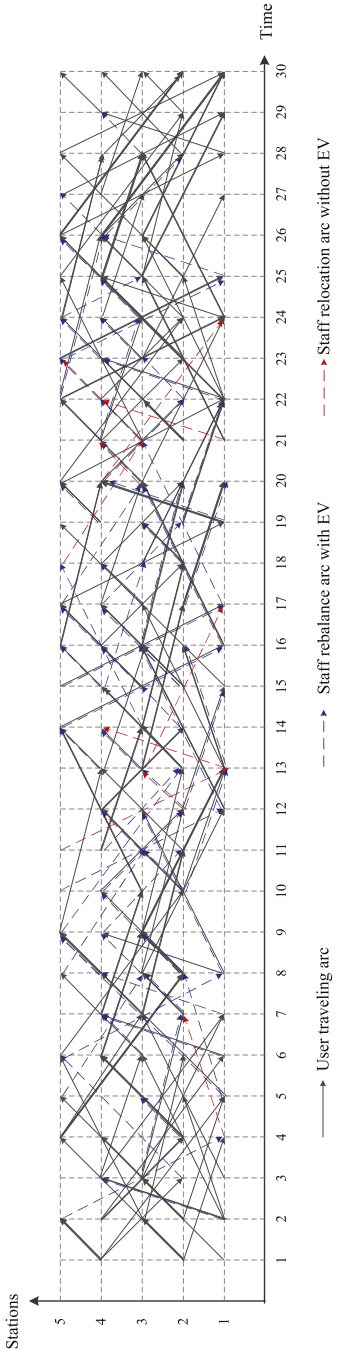

Fig. C.12. Computational results of a case in instance 5-30-200-40-20.

the experiment without considering the EV rebalancing operations. Specifically, we keep the EV and staff allocation plans, i.e., the values of $\{H_i\}_{i\in\mathbf{I}}$ and $\{F_i\}_{i\in\mathbf{I}}$. Then the user reservations are reassigned to the EVs based on the greedy algorithm (similar to the one adopted in Section 4.2), where the staff rebalancing operations are not considered. According to the experimental result, we find that the utility rates of EVs decrease from 78.57% to 61.19% and 15 users are no longer served.

Appendix D. LR approach with branch-and-bound

The detailed procedure of LR with branch-and-bound approach is described as follows. First, we obtain the initial solution by running the LR algorithm and then branch on variables $\mathbf{Y}$ in a depth-first manner. In specific, we first create a couple of initial lower and upper bounds by using the standard LR algorithm in Algorithm 5. Then we adopt a greedy heuristic to determine the branching rules: Define a set $\ddot{\mathbf{Y}}_k = \{Y^h_{it\,js} | Y^h_{it\,js} = 1\}$ to denote the assignment plan of EVs in iteration k. We choose variable $\dot{Y}^h_{it\,js}$ ($\dot{Y}^h_{it\,js} \in \ddot{\mathbf{Y}}_k$) as the next variable to be branched if the value of its corresponding Lagrangian multiplier $\dot{\mu}^h_{it\,js}$ is bigger than the others. In this way, two child nodes are obtained where the relaxed problem is solved with additional constraint $\dot{Y}^h_{it\,js} = 0$ in one node and $\dot{Y}^h_{it\,js} = 1$ in the other. Simultaneously, the upper bound shall be updated if a better feasible solution is found. In the bounding rules, we run the LR algorithm for a certain number (i.e., 10) of iterations at each newly generated child node to determine the lower and upper bounds. If the lower bound is higher than the best feasible solution so far, then no more branching is needed over this node, i.e., this branch can be safely pruned. Otherwise, update the upper bound when a better feasible solution is found and pass down the final multipliers to its child nodes as their initial multipliers. To balance the efficiency and accuracy of the solution algorithm in solving the real-word cases, we here terminate the branching process when the optimality gap G between the lower and upper bounds is smaller than 5% or the number of iterations is over 1000. Then output the best solution with optimality gap G.

Appendix E. Definition of performance indicators used in Section 5.3

The performance indicators used in Section 5.3 are defined as:

$$\text{EV amortized cost:} \quad C^H = c^a \sum_{i\in\mathbf{I}} H_i, \tag{34}$$

$$\text{Staff hiring cost:} \quad C^Y = c^y \sum_{i\in\mathbf{I}} F_i, \tag{35}$$

$$\text{EV traveling cost:} \quad C^L = \sum_{(i,t,j,s)\in\mathbf{A}} \sum_{h\in\mathbf{H}} c^l_{ij} X^h_{it\,js}, \tag{36}$$

$$\text{Staff relocation cost:} \quad C^D = \sum_{(i,t,j,s)\in\mathbf{A}} c^d_{ij} \Big(\sum_{f\in\mathbf{F}} Z^f_{it\,js} - \sum_{h\in\mathbf{H}} X^h_{it\,js} + N_{it\,js}\Big), \tag{37}$$

$$\text{Total cost:} \quad C = C^H + C^Y + C^L + C^D, \tag{38}$$

where the mathematical notations are the same as those in Section 3.

References

An, K., Ouyang, Y., 2016. Robust grain supply chain design considering post-harvest loss and harvest timing equilibrium. Transport. Res. Part E 88, 110–128.
An, S., Cui, N., Bai, Y., Xie, W., Chen, M., Ouyang, Y., 2015. Reliable emergency service facility location under facility disruption, en-route congestion and in-facility queuing. Transport. Res. Part E 82, 199–216.
Bai, Y., Ouyang, Y., Pang, J.S., 2016. Enhanced models and improved solution for competitive biofuel supply chain design under land use constraints. Eur. J. Oper. Res. 249 (1), 281–297.
Barth, M., Shaheen, S., 2002. Shared-use vehicle systesm: frameowork for classifying carsharing, station cars and combined approaches. Transport. Res. Rec. J.Transport. Res. Board 1791, 105–112.
Barth, M., Todd, M., Xue, L., 2004. User-based Vehicle Relocation Techniques for Multiple Station Shared-use Vehicle Systems. In: Proceedings of the 83th Annual Meeting of the Transportation Research Board. 2004.
Becker, H., Ciari, F., Axhausen, K.W., 2017. Comparing car-sharing schemes in switzerland: user groups and usage patterns. Transport. Res. Part A 97, 17–29.
Boland, N., Hewitt, M., Marshall, L., Savelsbergh, M., 2017. The continuous-time service network design problem. Oper. Res.. In press
Boyacı, B., Zografos, K., Geroliminis, N., 2015. An optimization framework for the development of efficient one-way car-sharing systems. Eur. J. Oper. Res. 240, 718–733.
Boyacı, B., Zografos, K., Geroliminis, N., 2017. An integrated optimization-simulation framework for vehicle and personal relocations of electric carsharing systems with reservations. Transport. Res. Part B 95, 214–237.
Bruglieri, M., Colorni, A., Lue, A., 2014. The vehicle relocation problem for the one-way electric vehicle sharing: an application to the milan case. Procedia - Soc. Behav. Sci. 111, 18–27.
Correia, G., Antunes, A., 2012. Optimization approach to depot location and trip selection in one-way carsharing systems. Transport. Res. Part E 48, 233–247.
Cui, J., Zhao, M., Li, X., Parsafard, M., An, S., 2016. Reliable design of an integrated supply chain with expedited shipments under disruption risks. Transport. Res. Part E 95, 143–163.
Dell'Amico, M., Hadjicostantinou, E., Iori, M., Novellani, S., 2014. The bike sharing rebalancing problem: mathematical formulations and benchmark instances. Omega (Westport) 45, 7–19.

Diabat, A., Battaia, O., Nazzal, D., 2015. An improved lagrangian relaxation-based heuristic for a joint location-inventory problem. Comp. Operat. Res. 61, 170–178.
Erdogan, S., Miller-Hooks, E., 2012. A green vehicle routing problem. Transport. Res. Part E 48 (1), 100–114.
Fanti, M.P., Mangini, A.M., Pedroncelli, G., Ukovich, W., 2014. Fleet sizing for electric car sharing system via closed queueing networks. IEEE Intern. Conf. Syst. ManCybernet. 2014, 1324–1329.
Febbraro, A., Sacco, N., Saeednia, M., 2012. One-way carsharing: solving the relocation problem. Transport. Res. Rec. J.Transport. Res. Board 2319, 113–120.
Firnkorn, J., 2012. Triangulation of two methods measuring the impacts of a free-floating carsharing system in germany. Transport. Res. Part A: PolicyPract. 46 (10), 1654–1672.
Fisher, M.L., 1981. The lagrangian relaxation method for solving integer programming problems. Manage. Sci. 27 (1), 1–18.
Fisher, M.L., Jörnsten, K.O., Madsen, O.B., 1997. Vehicle routing with time windows: two optimization algorithms. Oper. Res. 45 (3), 488–492.
Forma, I.A., Raviv, T., Tzur, M., 2015. A 3-step math heuristic for the static repositioning problem in bike-sharing systems. Transport.Res.Part B: Methodolog. 71, 230–247.
Fu, Y.M., Diabat, A., 2015. A lagrangian relaxation approach for solving the integrated quay crane assignment and scheduling problem. Appl. Math. Model. 39 (3), 1194–1201.
Furuhata, M., Dessouky, M., Ordóñez, F., Brunet, M.E., Wang, X., Koenig, S., 2013. Ridesharing: the state-of-the-art and future directions. Transport. Res. Part B 57, 28–46.
Geoffrion, A.M., 1974. Lagrangian relaxation for integer programming. Springer.
Hosni, H., Naoum-Sawaya, J., Artail, H., 2014. The shared-taxi problem: formulation and solution methods. Transport. Res. Part B 70, 303–318.
Hu, L., Liu, Y., 2016. Joint design of parking capacities and fleet size for one-way station-based carsharing systems with road congestion constraints. Transport. Res. Part B 93, 268–299.
Jian, S., Rashidi, T.H., Wijayaratna, K.P., Dixit, V.V., 2016. A spatial hazard-based analysis for modelling vehicle selection in station-based carsharing systems. Transport. Res. Part C 72, 130–142.
Jorge, D., Barnhart, C., de Almeida Correia, G.H., 2015. Assessing the viability of enabling a round-trip carsharing system to accept one-way trips: application to logan airport in boston. Transport. Res. Part C: Emerg.Technolog. 56, 359–372.
Jorge, D., Correia, G., Barnhart, C., 2014. Comparing optimal relocation operations with simulated relocation policies in one-way carsharing systems. IEEE Trans. Intell. Transp. Syst. 15 (4), 1667–1675.
Kek, A.G., Cheu, R.L., Meng, Q., Fung, C.H., 2009. A decision support system for vehicle relocation operations in carsharing systems. Transport. Res. Part E 45, 149–158.
Kliewer, N., Mellouli, T., Suhl, L., 2006. A time-space network based exact optimization model for multi-depot bus scheduling. Eur. J. Oper. Res. 175 (3), 1616–1627.
Kohl, N., Desrosiers, J., Madsen, O.B., Solomon, M.M., Soumis, F., 1999. 2-Path cuts for the vehicle routing problem with time windows. Transport. Sci. 33 (1), 101–116.
Li, P., Mirchandani, P., Zhou, X., 2015. Solving simultaneous route guidance and traffic signal optimization problem using space-phase-time hypernetwork. Transport. Res. Part B 81, 103–130.
Li, X., 2013. An integrated modeling framework for design of logistics networks with expedited shipment services. Transport. Res. Part E 56, 46–63.
Li, X., Ma, J., Cui, J., Ghiasi, A., Zhou, F., 2016. Design framework of large-scale one-way electric vehicle sharing systems: a continuum approximation model. Transport. Res. Part B 88, 21–45. MLA.
Li, X., Ouyang, Y., 2012. Reliable traffic sensor deployment under probabilistic disruptions and generalized surveillance effectiveness measures. Oper. Res. 60 (5), 1183–1198.
Liu, J., Zhou, X., 2016. Capacitated transit service network design with boundedly rational agents. Transport. Res. Part B 93, 225–250.
Lu, G., Zhou, X., Peng, Q., He, B., Mahmoudi, M., Zhao, J., 2016. Solving resource recharging station location-routing problem through a resource-space-time network representation. ArXiv preprint arXiv: 1602.06889.
Mahmoudi, M., Zhou, X., 2016. Finding optimal solutions for vehicle routing problem with pickup and delivery services with time windows: a dynamic programming approach based on state-space-time network representations. Transport. Res. Part B 89, 19–42.
Min, H., 1989. The multiple vehicle routing problem with simultaneous delivery and pick-up points. Transport. Res. Part A 23 (5), 377–386.
Nair, R., Miller-Hooks, E., 2011. Fleet management for vehicle sharing operations. Transport. Sci. 55 (4), 524–540.
Niu, H., Zhou, X., Tian, X., 2018. Coordinating assignment and routing decisions in transit vehicle schedules: a variable-splitting lagrangian decomposition approach for solution symmetry breaking. Transport. Res. Part B: Methodolog. 107, 70–101.
Nourinejad, M., Zhu, S., Bahrami, S., Roorda, M.J., 2015. Vehicle relocation and staff rebalancing in one-way carsharing systems. Transport. Res. Part E 81, 98–113.
Ouyang, Y., Wang, Z., Yang, H., 2015. Facility location design under continuous traffic equilibrium. Transport. Res. Part B 81, 18–33.
Schmöller, S., Weikl, S., Müller, J., Bogenberger, K., 2015. Empirical analysis of free-floating carsharing usage: the munich and berlin case. Transport. Res. Part C 56, 34–51.
Schneider, M., Stenger, A., Goeke, D., 2014. The electric vehicle-routing problem with time windows and recharging stations. Transport. Sci. 48 (4), 500–520.
Smith, S.L., Pavone, M., Schwager, M., Frazzoli, E., Rus, D., 2013. Rebalancing the rebalancers: optimally routing vehicles and drivers in mobility-on-demand systems. Am. Control Conf. 2013. 2362-236
Steinzen, I., Gintner, V., Suhl, L., Kliewer, N., 2010. A time-space network approach for the integrated vehicle and crew scheduling problem with multiple depots. Transport. Sci. 44 (3), 367–382.
Tong, L., Zhou, X., Miller, H.J., 2015. Transportation network design for maximizing space-time accessibility. Transport. Res. Part B 81, 555–576.
Tong, L.C., Zhou, L., Liu, J., Zhou, X., 2017. Customized bus service design for jointly optimizing passenger-to-vehicle assignment and vehicle routing. Transport. Res. Part C: Emerg.Technolog. 85, 451–475.
Toth, P., Vigo, D., 2014. Vehicle routing: Problems, methods, and applications. Soc. Indust. Appl. Math.
Waserhole, A., Jost, V., Brauner, N., 2013. Pricing techniques for self regulation in vehicle sharing systems. Electron. Notes Discrete Math. 41, 149–156.
Weikl, S., Bogenberger, K., 2015. A practice-ready relocation model for free-floating carsharing systems with electric vehicles - mesoscopic approach and field trail results. Transport. Res. Part C 57, 206–223.
Xu, M., Meng, Q., Liu, K., Yamamoto, T., 2017. Joint charging mode and location choice model for battery electric vehicle users. Transport. Res. Part B: Methodolog. 103, 68–86.
Xu, M., Meng, Q., Liu, Z., 2018. Electric vehicle fleet size and trip pricing for one-way carsharing services considering vehicle relocation and personnel assignment. Transport. Res. Part B: Methodolog. 111, 60–82.
Yang, L., Zhou, X., 2014. Constraint reformulation and a lagrangian relaxation-based solution algorithm for a least expected time path problem. Transport. Res. Part B 59, 22–44.
Yang, L., Zhou, X., 2017. Optimizing on-time arrival probability and percentile travel time for elementary path finding in time-dependent transportation networks: linear mixed integer programming reformulations. Transport. Res. Part B 96, 68–91.
Yin, J., Yang, L., Tang, T., Gao, Z., Ran, B., 2017. Dynamic passenger demand oriented metro train scheduling with energy-efficiency and waiting time minimization: mixed-integer linear programming approaches. Transport. Res. Part B 97, 182–213.
Zhang, D., Yu, C., Desai, J., Lau, H.Y.K., Srivathsan, S., 2016. A time-space network flow approach to dynamic repositioning in bicycle sharing systems. Transport. Res. Part B. In press.
Zhang, L., Meng, Q., Fwa, T.F., 2017. Big AIS data based spatial-temporal analyses of ship traffic in singapore port waters. Transport. Res. Part E: Logist.Transport. Rev. In press.